FLUOROCARBON ETCHING OF POROUS SILICON DIOXIDE: PLASMA CHEMISTRY AND SURFACE KINETICS

Arvind Sankaran, Alex Vasenkov and Mark J. Kushner
University of Illinois
Department of Electrical and Computer Engineering
Urbana, IL 61801
mjk@uiuc.edu http://uigelz.ece.uiuc.edu

October 2002

AGENDA AND ACKNOWLEDGEMENTS

- Fluorocarbon plasma etching of dielectrics
- Description of modeling hierarchy
- Scaling laws for solid and porous dielectric etching
- Concluding Remarks
- Acknowledgements:
    - Prof. Gottlieb Oehrlein
    - Semiconductor Research Corporation, National Science Foundation, Sematech, Applied Materials

FLUOROCARBON PLASMA ETCHING: DIELECTRICS

- **Fluorocarbon plasma etching of dielectrics, and selectivity with respect to conductors, is one of the first plasma processing technologies.**

- **Earliest works of Coburn and Winters addressed CF_4 etching of Si and SiO_2.**

- **In spite of longevity, fluorocarbon plasma etching is still the foremost process for obtaining selectivity between dielectrics (e.g., SiO_2, Si_3N_4) and underlying conductors (e.g., Si, p-Si).**

- **Optimization of these processes is critical as dielectrics thin and selectivity requirements become extreme.**

- **The use of low-k dielectrics for interconnect wiring with new materials has brought new challenges.**

FLUORCARBON PLASMA ETCHING: SELECTIVITY

- **Selectivity in fluorocarbon etching relies on polymer deposition.**
- **Electron impact dissociation of feedstock fluorocarbons produce polymerizing radicals and ions, resulting in polymer deposition.**

$$e + Ar/C_4F_8 \longrightarrow CF_n, M^+$$

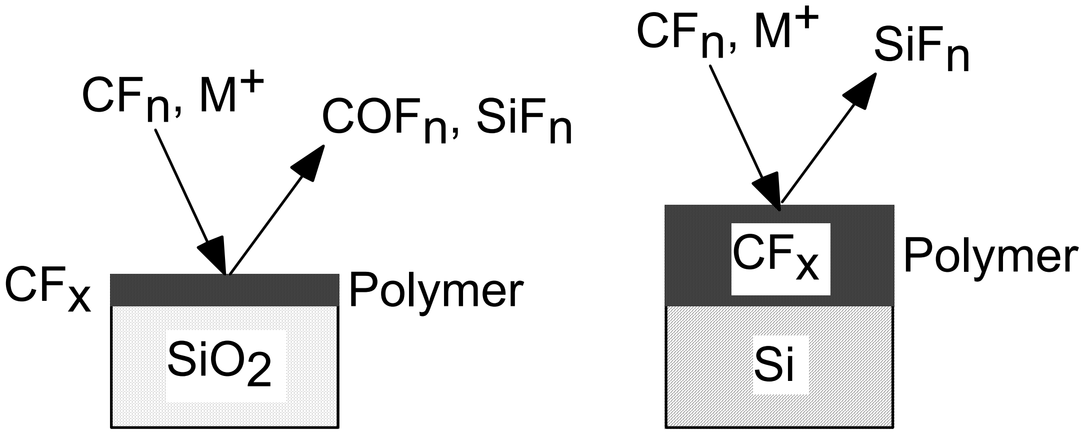

- **Compound dielectrics contain oxidants which consume the polymer, producing thinner polymer layers.**
- **Thicker polymer on non-dielectrics restrict delivery of ion energy (lower etching rates).**

FLUORCARBON PLASMA ETCHING: SELECTIVITY

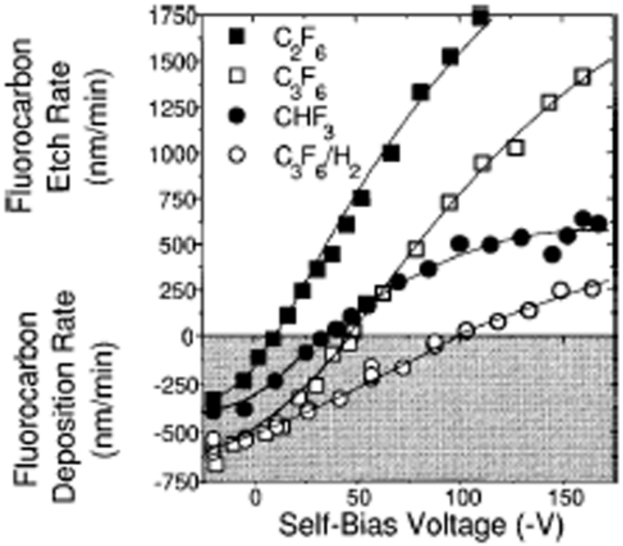

- **Low bias: Deposition**
- **High bias: etching**

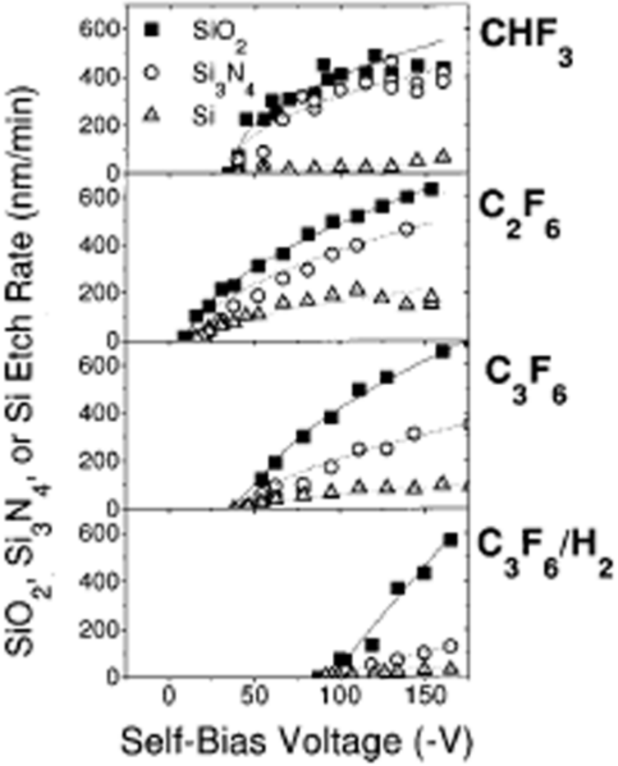

- **Etch Rate (SiO_2 > Si)**

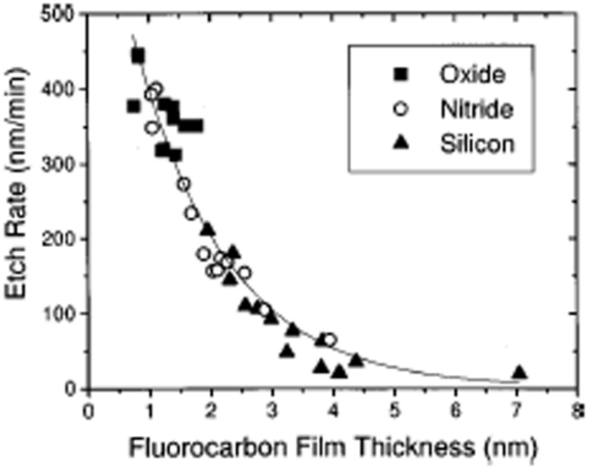

- **Polymer Thickness (SiO_2 < Si)**

- **G. Oerhlein, et al., JVSTA 17, 26 (1999)**

PLASMA ETCHING OF LOW-K DIELECTRICS

- **Low dielectric constant (low-k) dielectrics are generally classified as inorganic, organic or hybrid.**

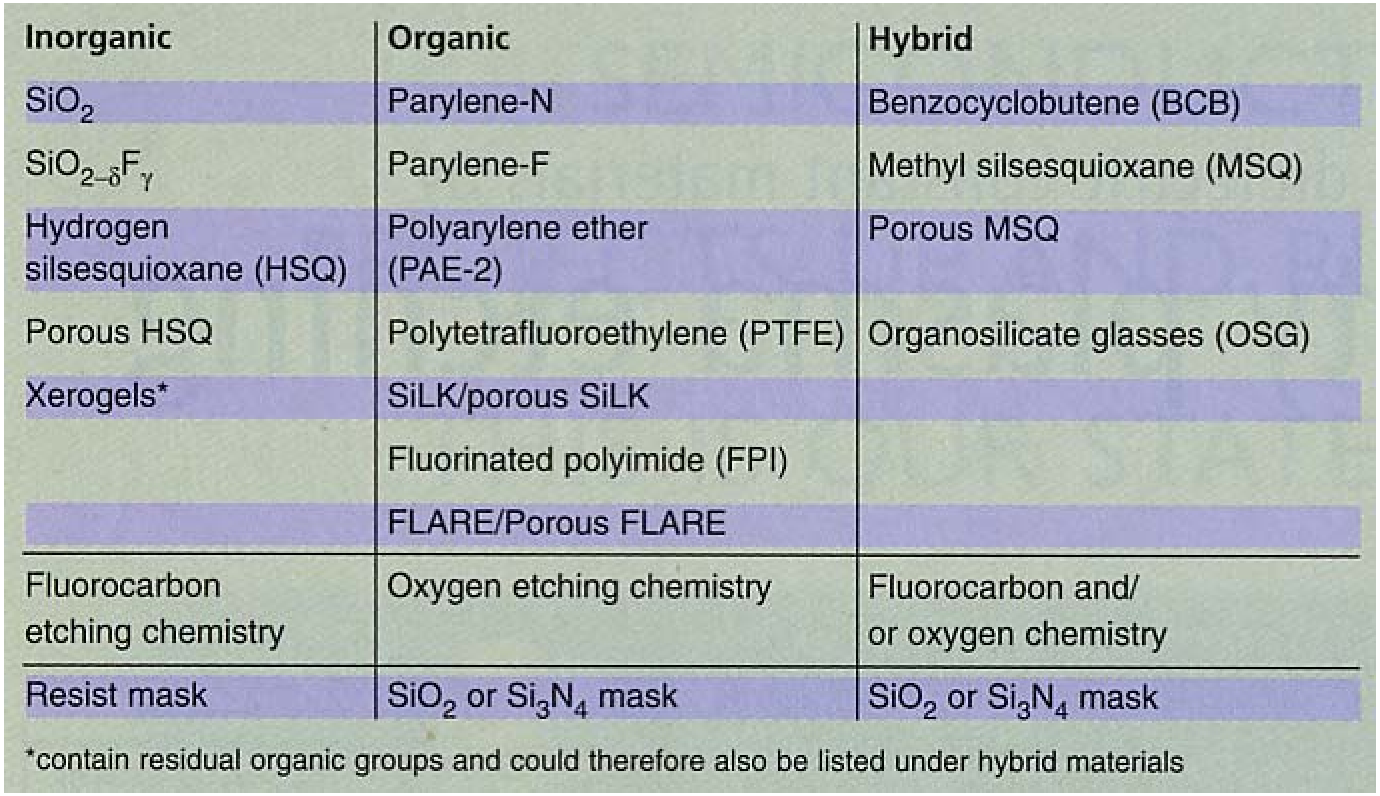

Inorganic	Organic	Hybrid
SiO_2	Parylene-N	Benzocyclobutene (BCB)
$SiO_{2-\delta}F_{\gamma}$	Parylene-F	Methyl silsesquioxane (MSQ)
Hydrogen silsesquioxane (HSQ)	Polyarylene ether (PAE-2)	Porous MSQ
Porous HSQ	Polytetrafluoroethylene (PTFE)	Organosilicate glasses (OSG)
Xerogels*	SiLK/porous SiLK	
	Fluorinated polyimide (FPI)	
	FLARE/Porous FLARE	
Fluorocarbon etching chemistry	Oxygen etching chemistry	Fluorocarbon and/ or oxygen chemistry
Resist mask	SiO_2 or Si_3N_4 mask	SiO_2 or Si_3N_4 mask

*contain residual organic groups and could therefore also be listed under hybrid materials

- **Inorganics are etched using fluorocarbon chemistries; organics are etched using oxygen chemistries.**

  - **Solid State Technology, May 2000**

POROUS SILICON DIOXIDE

- Porous SiO_2 (xerogels) have low-k properties due to their lower mass density resulting from (vacuum) pores.

    - Typical porosities: 30-70%
    - Typical pore sizes: 2-20 nm

- Porous SiO_2 (P-SiO_2) is, from a process development viewpoint, an ideal low-k dielectric.

    - Extensive knowledge base for fluorocarbon etching of conventional non-porous (NP-SiO_2).

    - No new materials (though most P-SiO_2 contains some residual organics)

    - Few new integration requirements

ETCHING OF P-SiO_2: GENERAL TRENDS

- Etching of Porous SiO_2 typically proceeds at a higher rate than NP-SiO_2 for the same conditions due to the lower mass density.

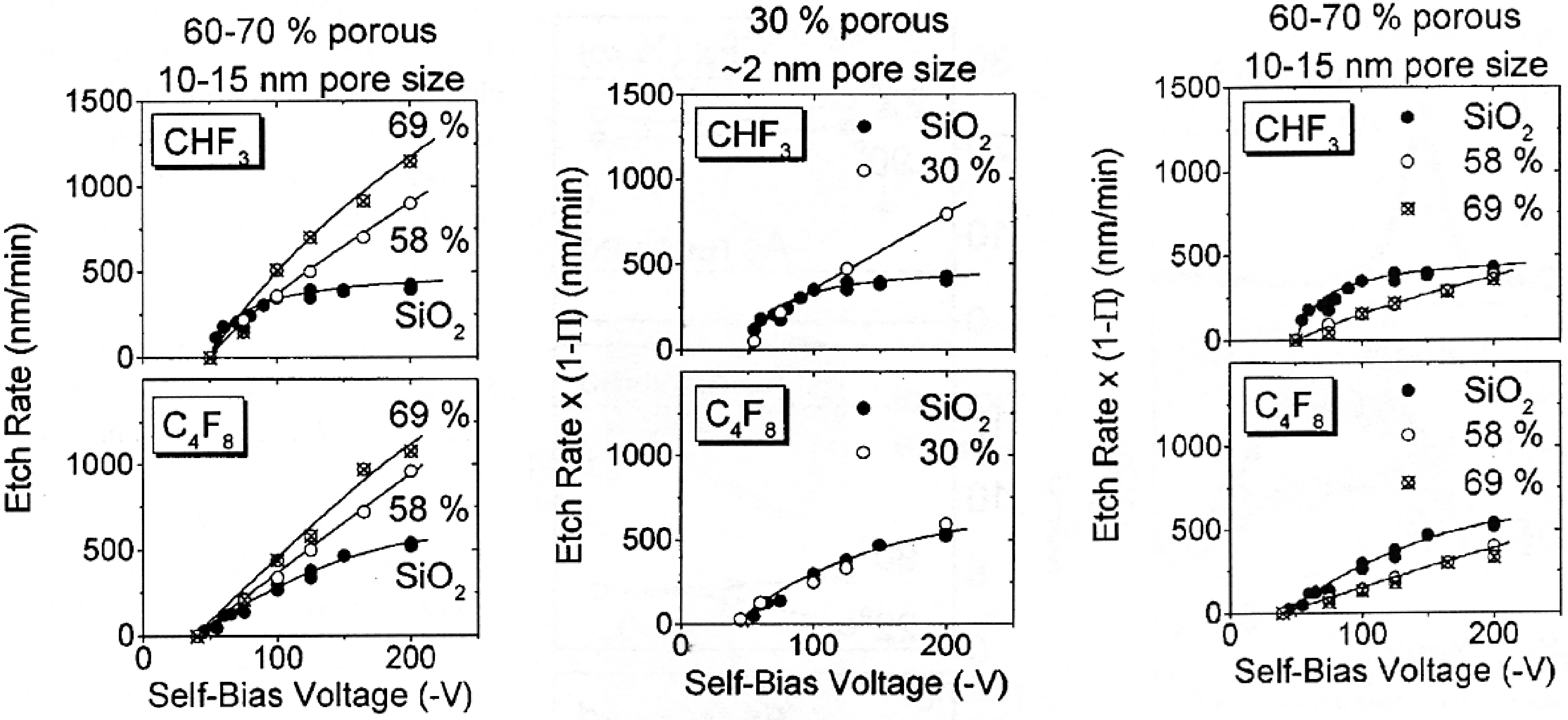

- When correcting for mass, etch rates are either larger or smaller than NP- SiO_2, depending on porosity, pore size, polymerization.

  - Standaert et al, JVSTA 18, 2742 (2000).

MODELING OF FLUOROCARBON PLASMA ETCHING

- **Our research group has developed an integrated reactor and feature scale modeling hierarchy to model plasma processing systems.**

  - **<u>HPEM (Hybrid Plasma Equipment Model)</u>**
    - **Reactor scale**
    - **2- and 3-dimensional**
    - **ICP, CCP, MERIE, ECR**
    - **Surface chemistry**
    - **First principles**

  - **<u>MCFPM (Monte Carlo Feature Profile Model)</u>**
    - **Feature scale**
    - **2- and 3-dimensional**
    - **Fluxes from HPEM**
    - **First principles**

HYBRID PLASMA EQUIPMENT MODEL

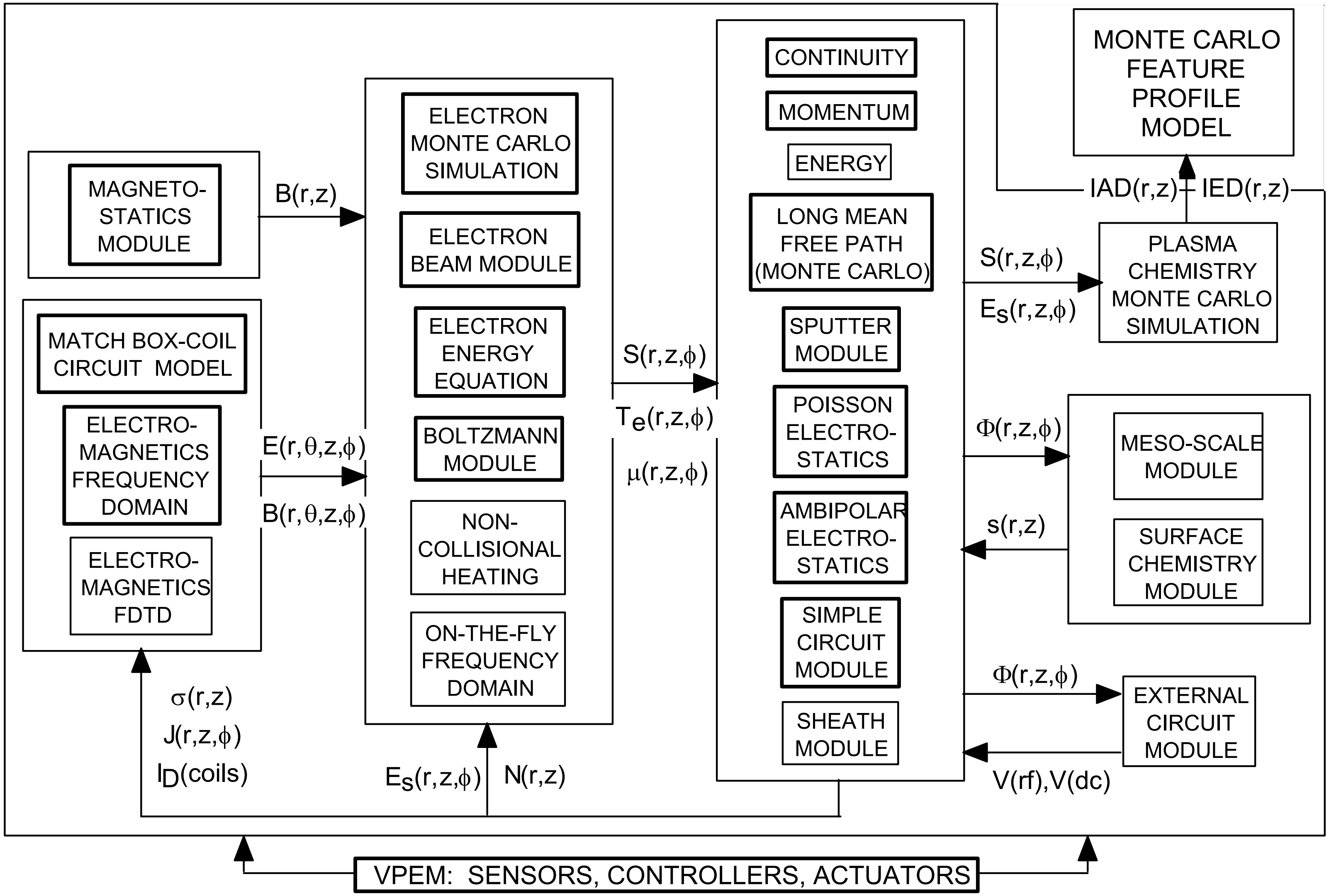

MAGNETO-STATICS MODULE

$B(r,z)$

MATCH BOX-COIL CIRCUIT MODEL

ELECTRO-MAGNETICS FREQUENCY DOMAIN

ELECTRO-MAGNETICS FDTD

$E(r,\theta,z,\phi)$

$B(r,\theta,z,\phi)$

ELECTRON MONTE CARLO SIMULATION

ELECTRON BEAM MODULE

ELECTRON ENERGY EQUATION

BOLTZMANN MODULE

NON-COLLISIONAL HEATING

ON-THE-FLY FREQUENCY DOMAIN

$S(r,z,\phi)$

$T_e(r,z,\phi)$

$\mu(r,z,\phi)$

CONTINUITY

MOMENTUM

ENERGY

LONG MEAN FREE PATH (MONTE CARLO)

SPUTTER MODULE

POISSON ELECTRO-STATICS

AMBIPOLAR ELECTRO-STATICS

SIMPLE CIRCUIT MODULE

SHEATH MODULE

$\sigma(r,z)$

$J(r,z,\phi)$

I_D(coils)

$E_s(r,z,\phi)$

$N(r,z)$

MONTE CARLO FEATURE PROFILE MODEL

IAD(r,z) IED(r,z)

PLASMA CHEMISTRY MONTE CARLO SIMULATION

$S(r,z,\phi)$

$E_s(r,z,\phi)$

$\Phi(r,z,\phi)$

$s(r,z)$

MESO-SCALE MODULE

SURFACE CHEMISTRY MODULE

$\Phi(r,z,\phi)$

V(rf),V(dc)

EXTERNAL CIRCUIT MODULE

VPEM: SENSORS, CONTROLLERS, ACTUATORS

ELECTROMAGNETICS MODEL

- **The wave equation is solved in the frequency domain using sparse matrix techniques (2D,3D):**

$$-\nabla\left(\frac{1}{\mu}\nabla\cdot\overline{E}\right)+\nabla\cdot\left(\frac{1}{\mu}\nabla\overline{E}\right)=\frac{\partial^2\left(\varepsilon\overline{E}\right)}{\partial t^2}+\frac{\partial\left(\overline{\overline{\sigma}}\cdot\overline{E}+\overline{J}\right)}{\partial t}$$

$$\vec{E}(\vec{r},t)=\vec{E}'(\vec{r})\exp(-i(\omega t+\varphi(\vec{r})))$$

- **Conductivities are tensor quantities (2D,3D):**

$$\overline{\overline{\sigma}}=\sigma_o\frac{m\nu_m}{q\alpha}\frac{1}{\left(\alpha^2+\left|\vec{B}\right|^2\right)}\begin{pmatrix}\alpha^2+B_r^2 & \alpha B_z+B_rB_\theta & -\alpha B_\theta+B_rB_z\\ -\alpha B_z+B_rB_\theta & \alpha^2+B_\theta^2 & \alpha B_r+B_\theta B_z\\ -\alpha B_\theta+B_rB_z & -\alpha B_r+B_\theta B_z & \alpha^2+B_z^2\end{pmatrix}$$

$$\vec{j}=\overline{\overline{\sigma}}\cdot\vec{E}\qquad\qquad\alpha=\frac{\left(i\omega+\nu_m\right)}{q/m},\quad\sigma_o=\frac{q^2n_e}{m\nu_m}$$

ELECTRON ENERGY TRANSPORT

- **Continuum (2D,3D):**

$$\partial\left(\frac{3}{2}n_e k T_e\right)/\partial t = S(T_e) - L(T_e) - \nabla\cdot\left(\frac{5}{2}\Phi k T_e - \overline{\overline{\kappa}}(T_e)\cdot\nabla T_e\right) + S_{EB}$$

where $S(T_e)$ = Power deposition from electric fields
$L(T_e)$ = Electron power loss due to collisions
Φ = Electron flux
$\kappa(T_e)$ = Electron thermal conductivity tensor
S_{EB} = Power source source from beam electrons

- **Power deposition has contributions from wave and electrostatic heating.**

- **Kinetic (2D,3D): A Monte Carlo Simulation is used to derive $f(\varepsilon,\vec{r},t)$ including electron-electron collisions using electromagnetic fields from the EMM and electrostatic fields from the FKM.**

PLASMA CHEMISTRY, TRANSPORT AND ELECTROSTATICS

- **Continuity, momentum and energy equations are solved for each species (with jump conditions at boundaries) (2D,3D).**

$$\frac{\partial N_i}{\partial t} = -\nabla \cdot (N_i \vec{\mathrm{v}}_i) + S_i$$

$$\frac{\partial \left(N_i \vec{v}_i\right)}{\partial t} = \frac{1}{m_i}\nabla\left(kN_iT_i\right) - \nabla \cdot \left(N_i \vec{v}_i \vec{v}_i\right) + \frac{q_i N_i}{m_i}\left(\vec{E} + \vec{v}_i \times \vec{B}\right) - \nabla \cdot \overline{\mu}_i - \sum_j \frac{m_j}{m_i + m_j} N_i N_j \left(\vec{v}_i - \vec{v}_j\right)\nu_{ij}$$

$$\frac{\partial \left(N_i \varepsilon_i\right)}{\partial t} + \nabla \cdot \mathrm{Q}_i + P_i \nabla \cdot \mathrm{U}_i + \nabla \cdot (N_i \mathrm{U}_i \varepsilon_i) = \frac{N_i q_i^2 \nu_i}{m_i(\nu_i^2 + \omega^2)} E^2 + \frac{N_i q_i^2}{m_i \nu_i} E_s^2 + \sum_j 3 \frac{m_{ij}}{m_i + m_j} N_i N_j R_{ij} k_B (T_j - T_i) \pm \sum_j 3 N_i N_j R_{ij} k_B T_j$$

- **Implicit solution of Poisson’s equation (2D,3D):**

$$\nabla \cdot \varepsilon \nabla \Phi\left(t + \Delta t\right) = -\left(\rho_s + \sum_i q_i N_i - \Delta \mathrm{t} \cdot \sum_{\mathrm{i}} \left(\mathrm{q}_{\mathrm{i}} \nabla \cdot \vec{\phi}_i\right)\right)$$

MONTE CARLO FEATURE PROFILE MODEL (MCFPM)

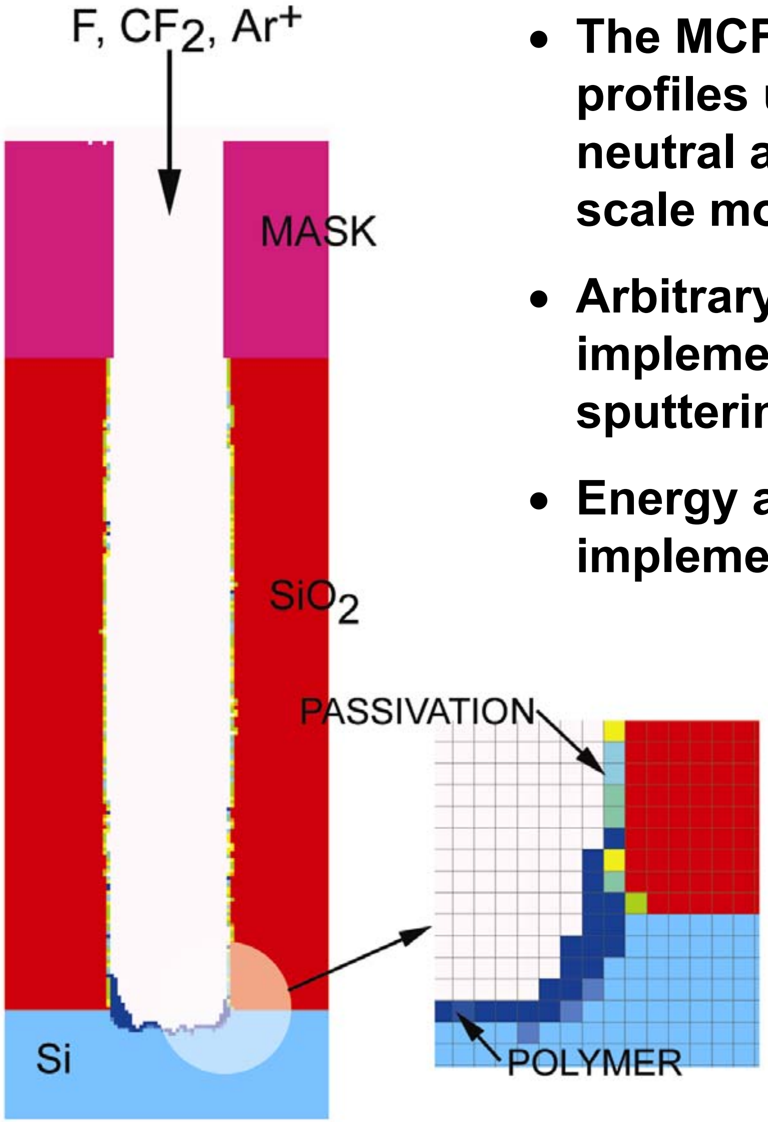

- The MCFPM predicts time and spatially dependent profiles using energy and angularly resolved neutral and ion fluxes obtained from equipment scale models.
- Arbitrary chemical reaction mechanisms may be implemented, including thermal and ion assisted, sputtering, deposition and surface diffusion.
- Energy and angular dependent processes are implemented using parametric forms.
- Mesh centered identify of materials allows "burial", overlayers and transmission of energy through materials.

University of Illinois
Optical and Discharge Physics

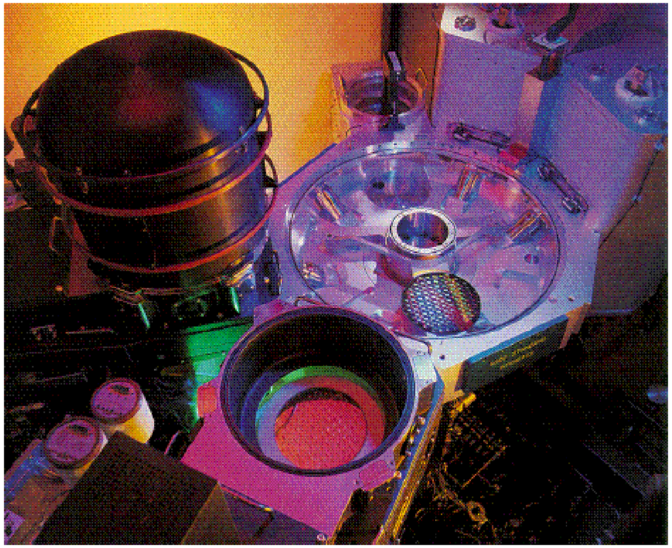

rf BIASED INDUCTIVELY COUPLED PLASMAS

- **Inductively Coupled Plasmas (ICPs) with rf biasing are used here.**
- **< 10s mTorr, 10s MHz, 100s W – kW, electron densities of 10^{11}-10^{12} cm^{-3}.**

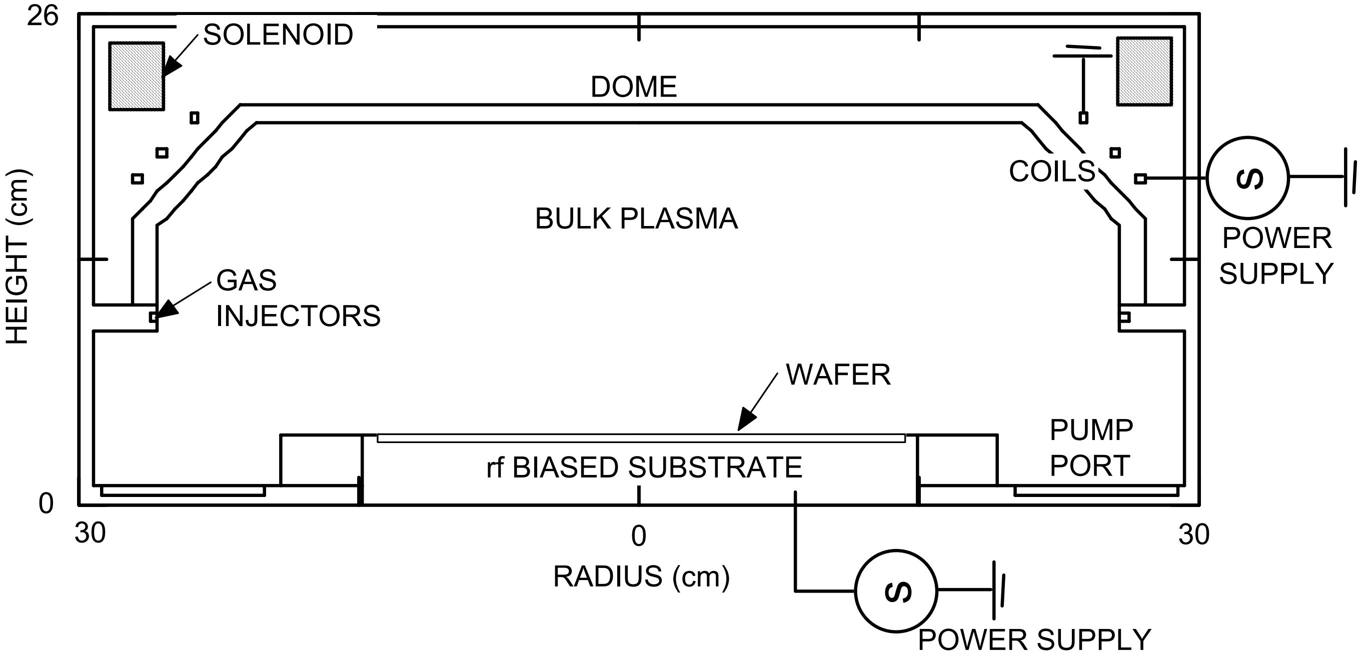

University of Illinois
Optical and Discharge Physics

TYPICAL ICP CONDITIONS: [e] FOR C_4F_8, 10 mTORR

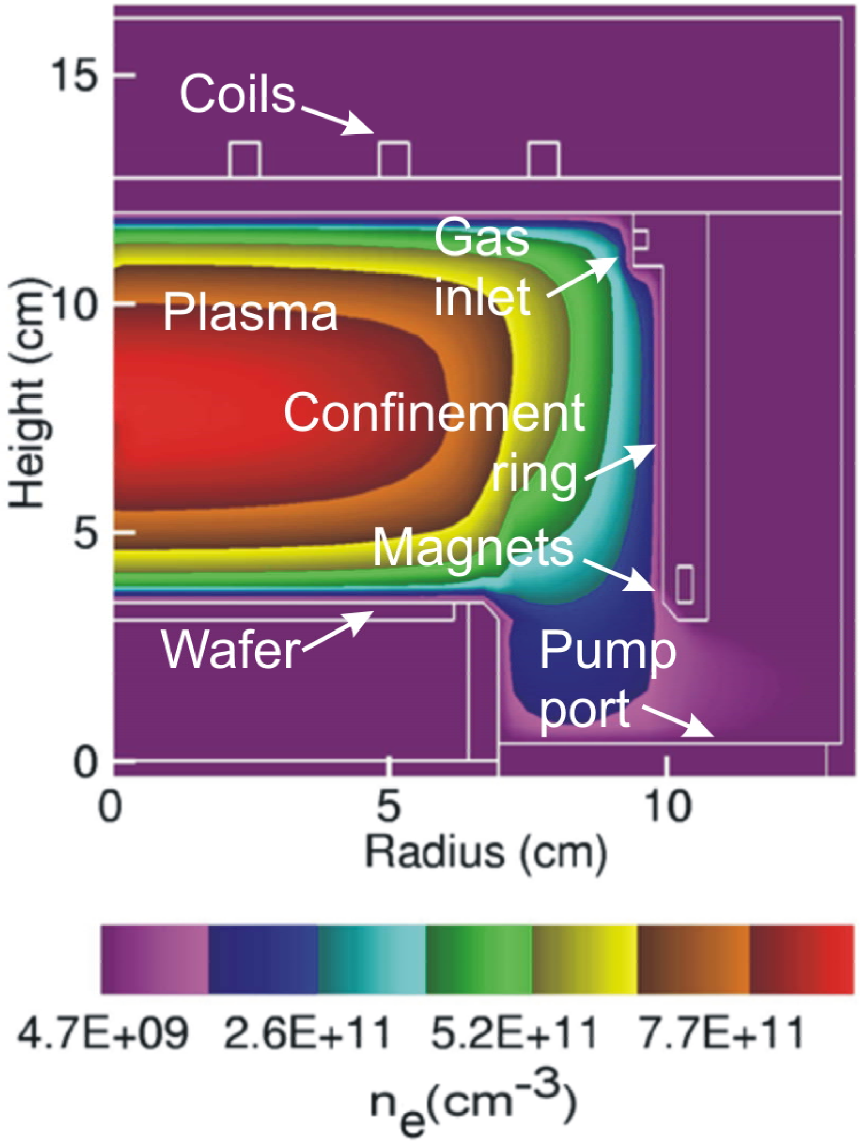

- An ICP reactor patterned after Oeherlein, et al. was used for validation.
- Reactor uses 3-turn coil (13.56 MHz) with rf biased substrate (3 MHz)
- Electron densities are 10^{11}-10^{12} cm^{-3} for 1.4 kW.

POWER, C_4F_8 DENSITY

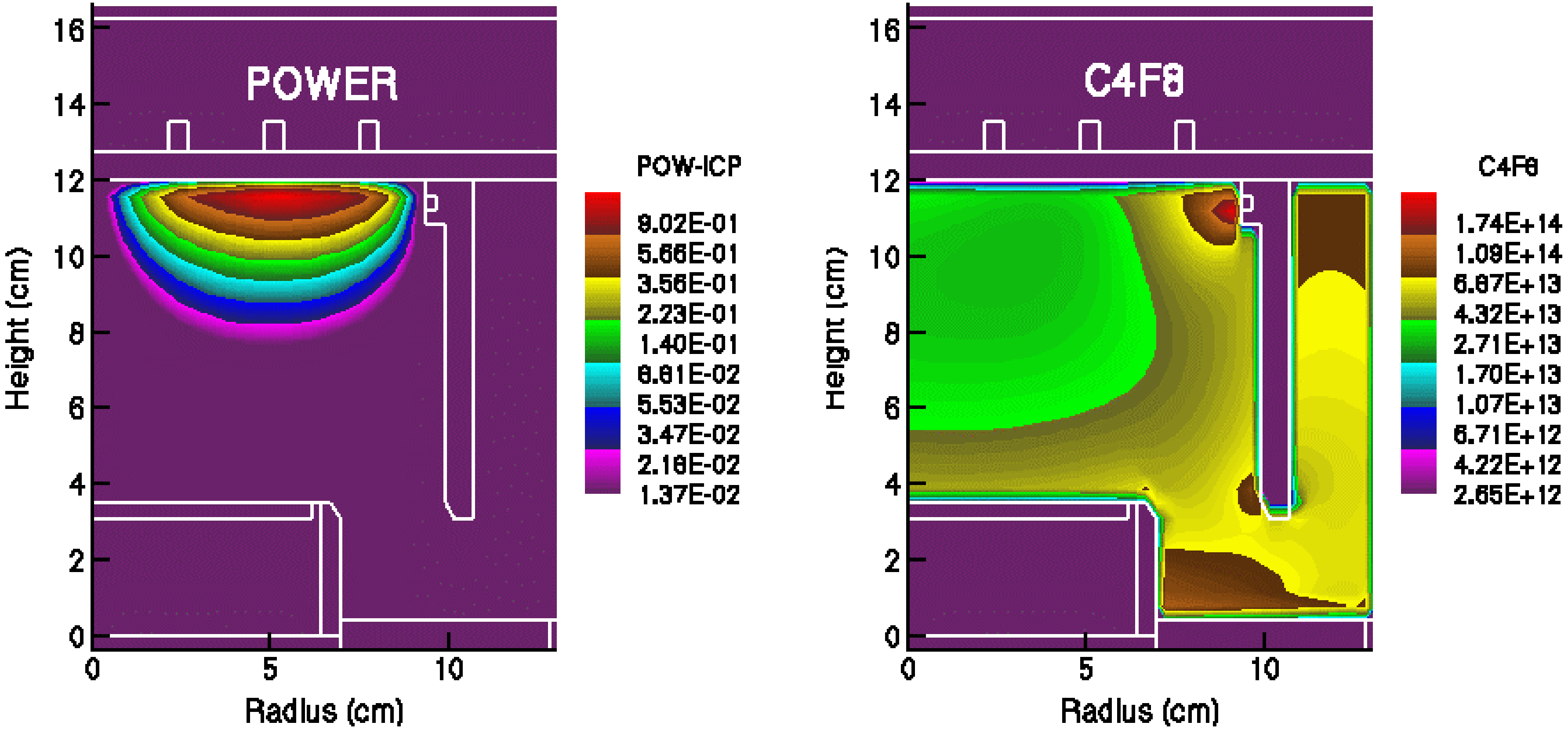

- **Large power deposition typically results in near total dissociation of feedstock gases.**

- **C_4F_8, 10 mTorr, 1.4 kW, 13.56 MHz**

ADVMET_1002_12

MAJOR POSITIVE IONS: C_4F_8, 10 mTORR

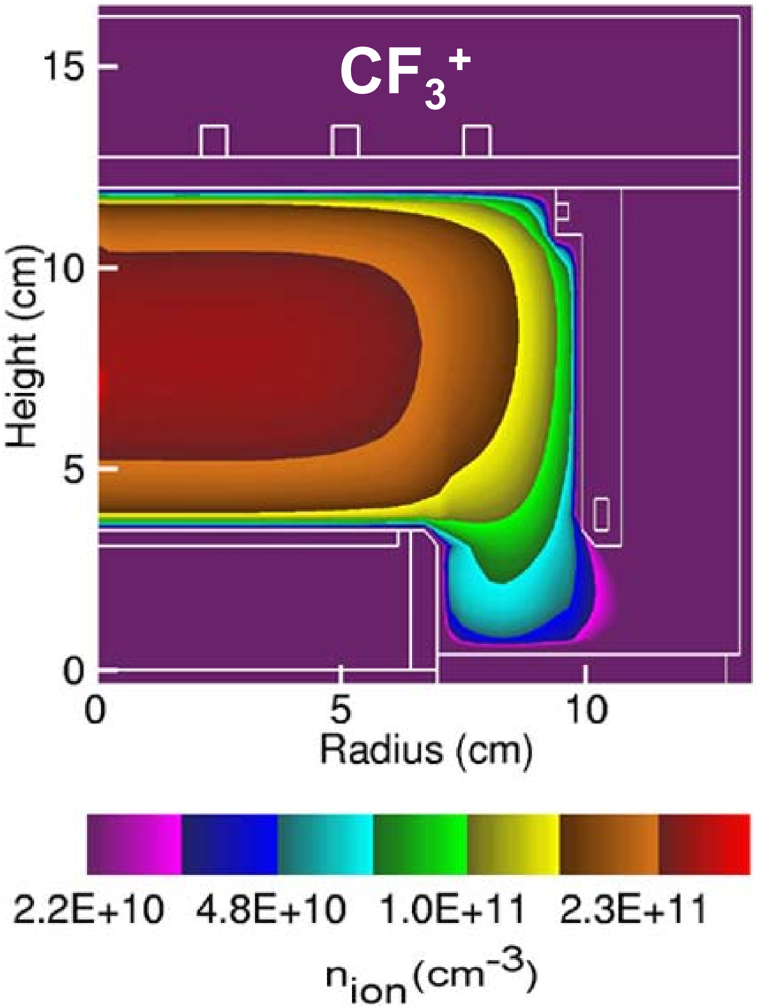

- CF_3^+, CF_2^+, and CF^+ are dominant ions due to dissociation of C_4F_8.

- C_4F_8, 10 mTorr, 1.4 kW, 13.56 MHz

CF_3^+ TEMPERATURE

- **The ion temperature is peaked near the walls where ions gain energy during acceleration in the presheath.**

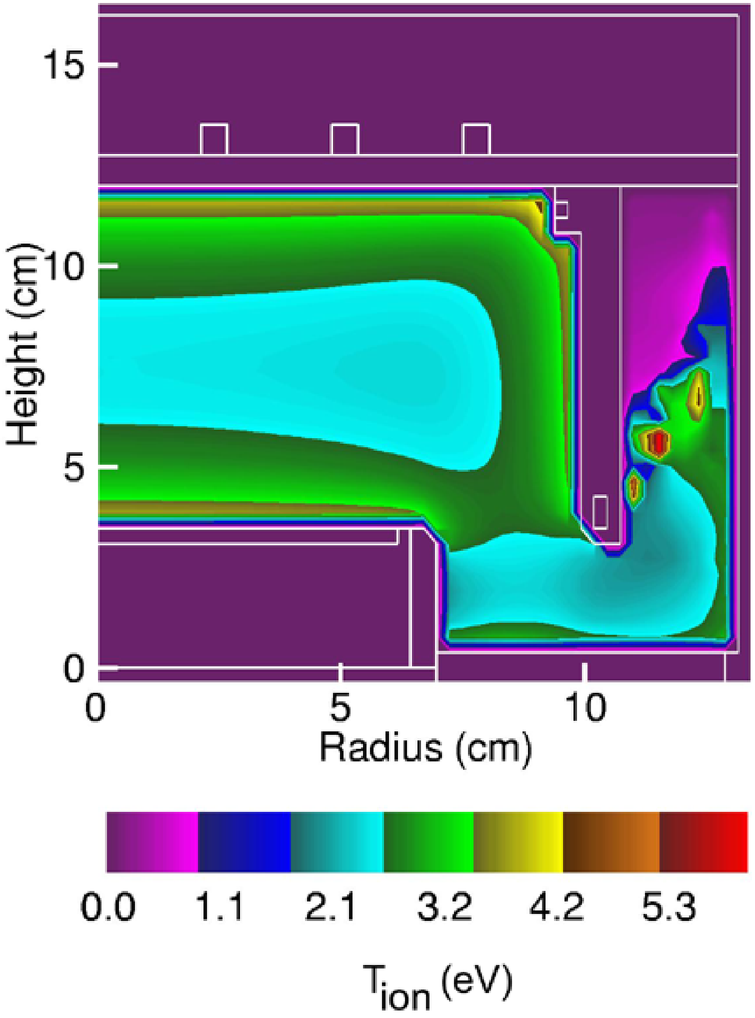

- **C_4F_8, 10 mTorr, 1.4 kW, 13.56 MHz**

I_P VERSUS ICP POWER for C_4F_8

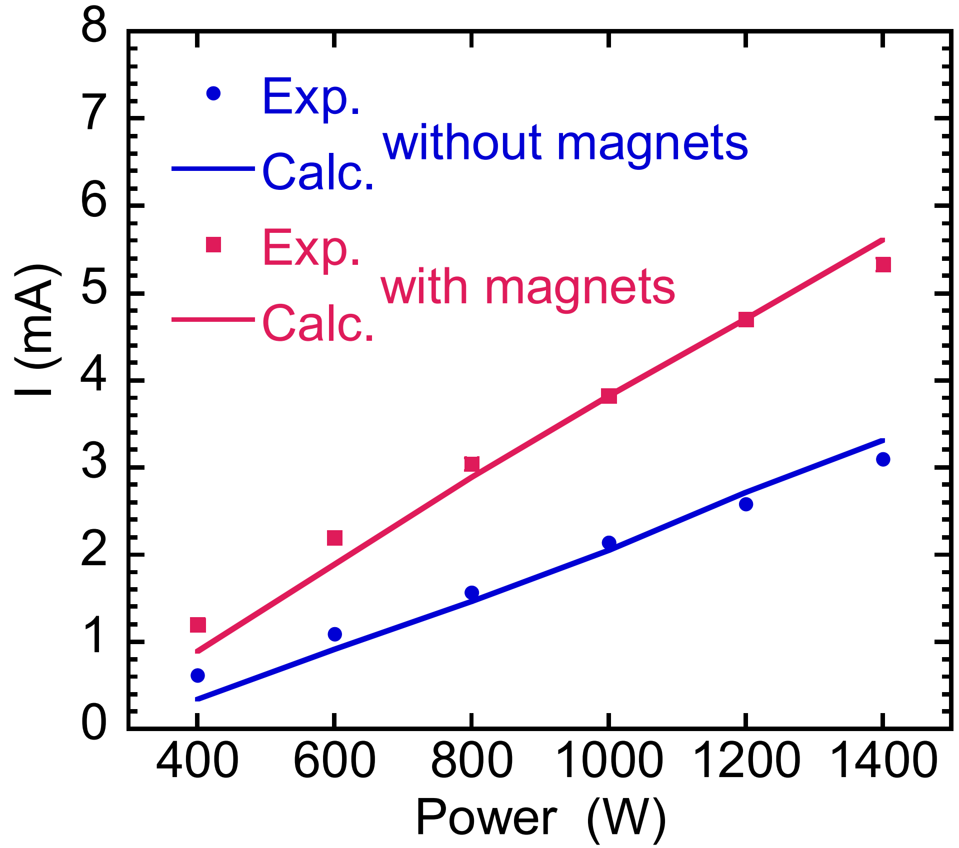

- **Extensive validation of the plasma models are performed with available data for densities, temperatures and fluxes.**

- **Ion saturation current derived from the model are compared to experiments: Ion densities are larger with moderate static magnetic fields.**

- **C_4F_8, 10 mTorr, 13.56 MHz, 100 V probe bias**

- **Experiments: G. Oehrlein, Private Comm.**

ION/NEUTRAL ENERGY/ANGULAR DISTRIBUTIONS

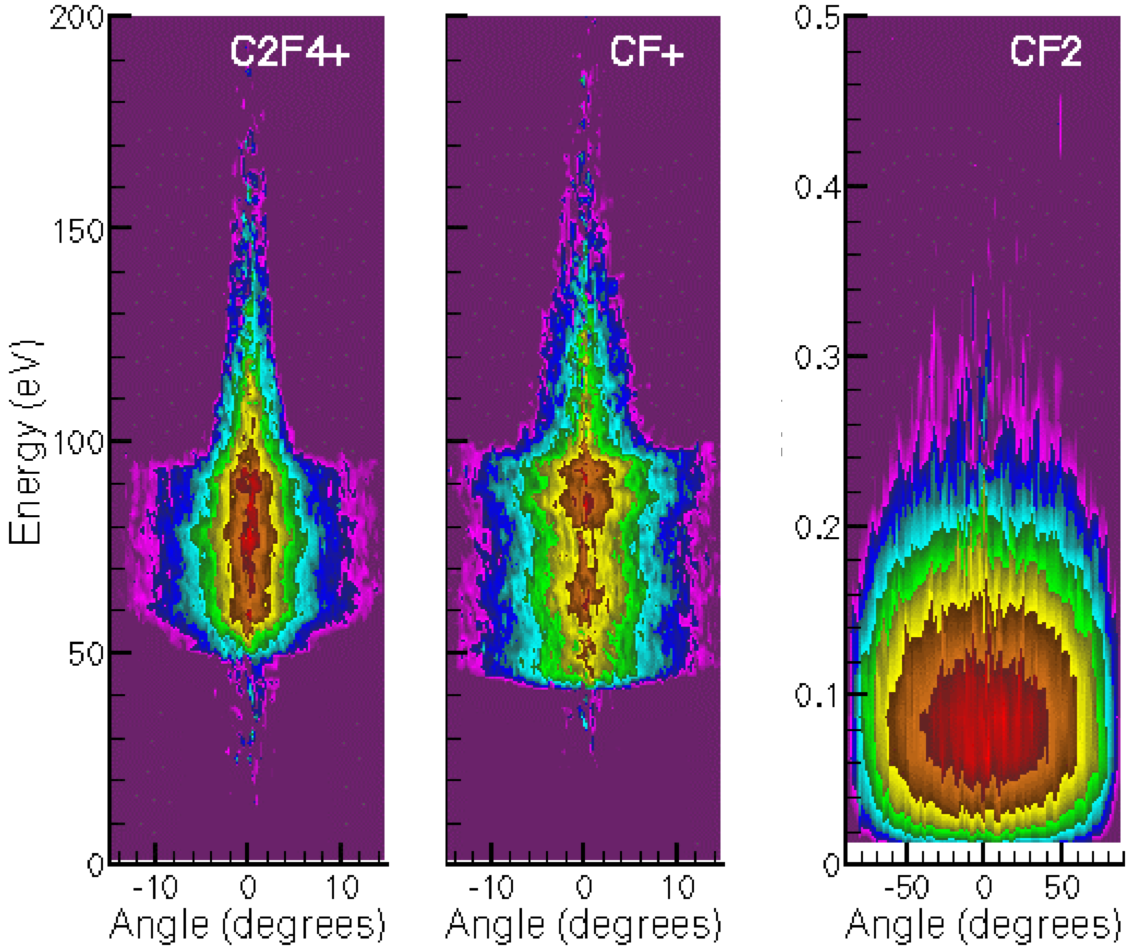

- The end products of reactor scale modeling are energy and ion angular distributions to the surface.
- In complex gas mixtures the IEADs can significantly vary from species to species.

- Ar/C_4F_8, 40 mTorr, 10b MHz, MERIE

SURFACE KINETICS DURING Si/SiO_2 ETCHING

- **Fluorocarbon etching of SiO_2 relies on a polymerization and chemically enhanced sputtering.**
- **C_xF_y passivation regulates delivery of precursors and activation energy.**
- **Chemisorption of CF_x produces a complex at the oxide-polymer interface.**
- **2-step ion activated (through polymer layer) etching of the complex consumes the polymer. Activation scales inversely with polymer thickness.**

- **Etch precursors and products diffuse through the polymer layer.**
- **In Si etching, CF_x is not consumed, resulting in thicker polymer layers.**

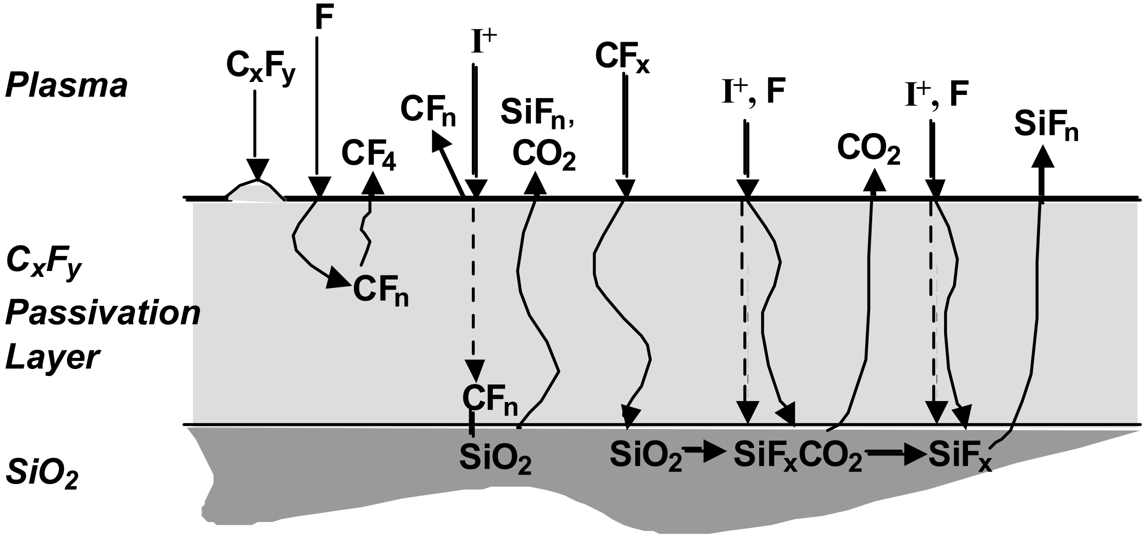

ETCH RATES AND POLYMER THICKNESS

- **Etch rates for Si and SiO_2 increase with increasing bias due, in part, to a decrease in polymer thickness.**
- **The polymer is thinner with SiO_2 due to its consumption during etching, allowing for more efficient energy transfer through the layer and more rapid etching.**

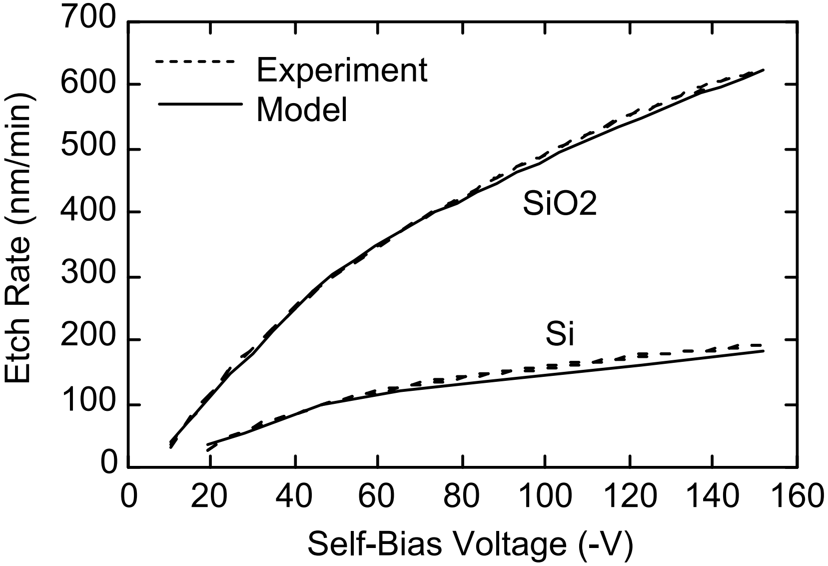

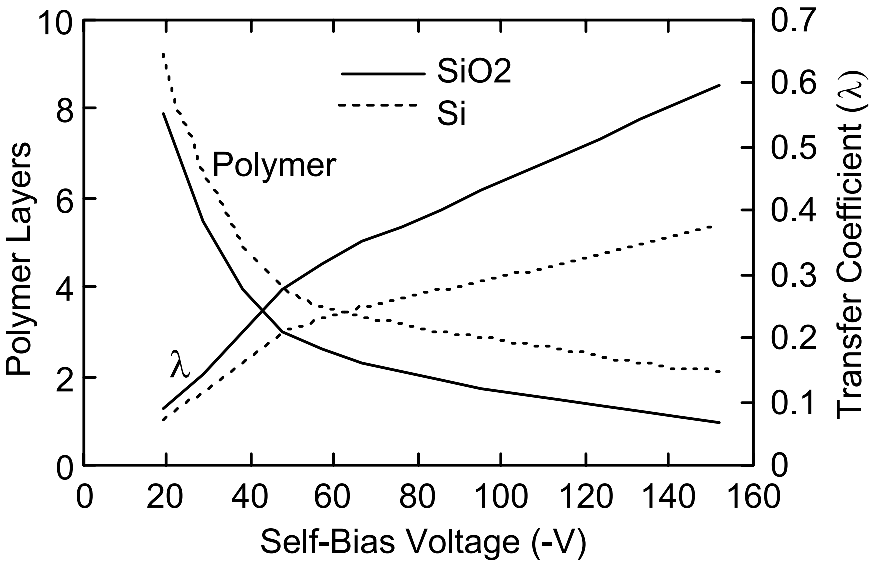

- **C_2F_6, 6 mTorr, 1400 W ICP, 40 sccm**
- **Exp. Ref: T. Standaert, et al.**
  J. Vac. Sci. Technol. A 16, 239 (1998).

POLYMERIZATION AIDS SELECTIVITY

- Less consumption of polymer on Si relative to SiO_2 slows and, in some cases, terminates etching, providing high selectivity.

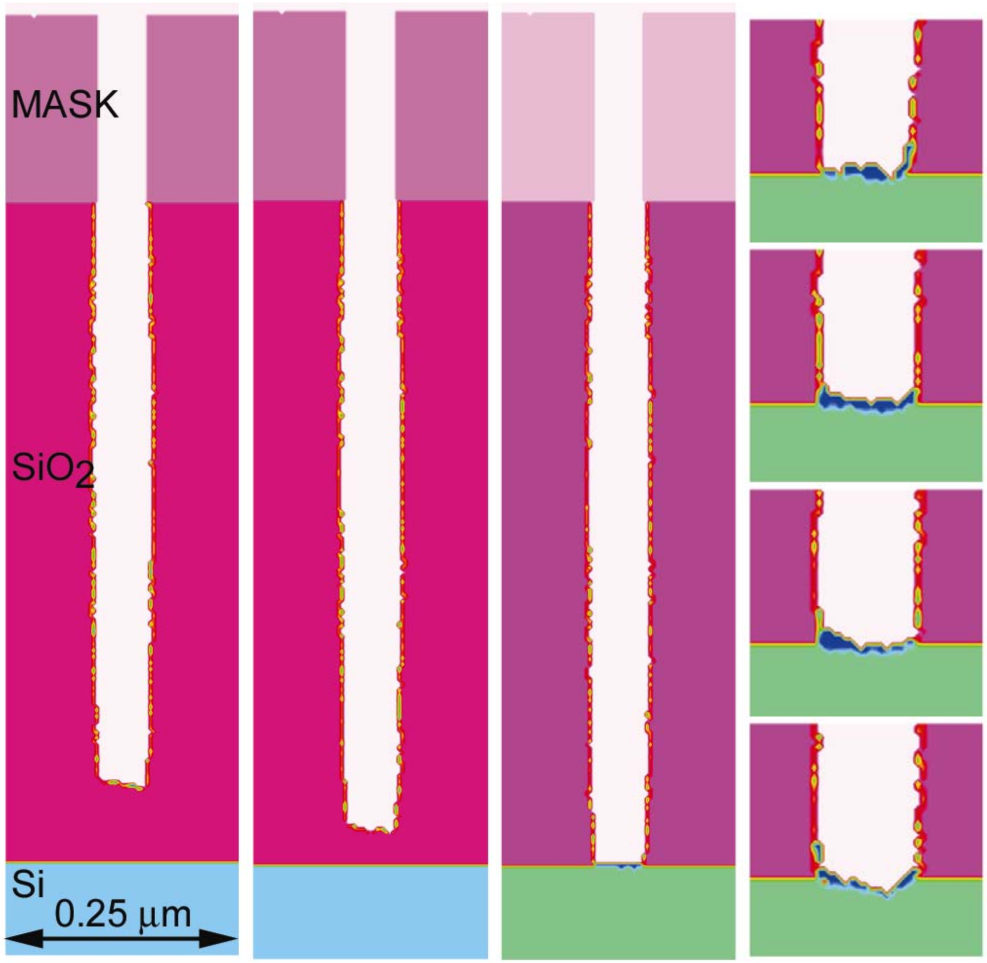

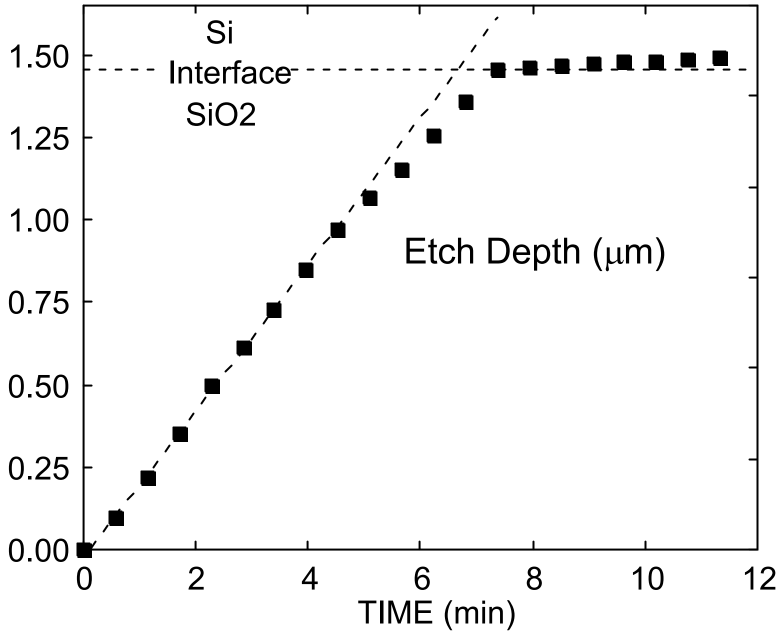

TAPERED AND BOWED PROFILES

- In high aspect ratio (HAR) etching of SiO_2 the sidewall of trenches are passivated by neutrals (CF_x, $x \leq 2$) due to the broad angular distributions of neutral fluxes.

- Either tapered or bowed profiles can result from a non-optimum combination of processing parameters including:

    - Degree of passivation
    - Ion energy distribution
    - Radical/ion flux composition.

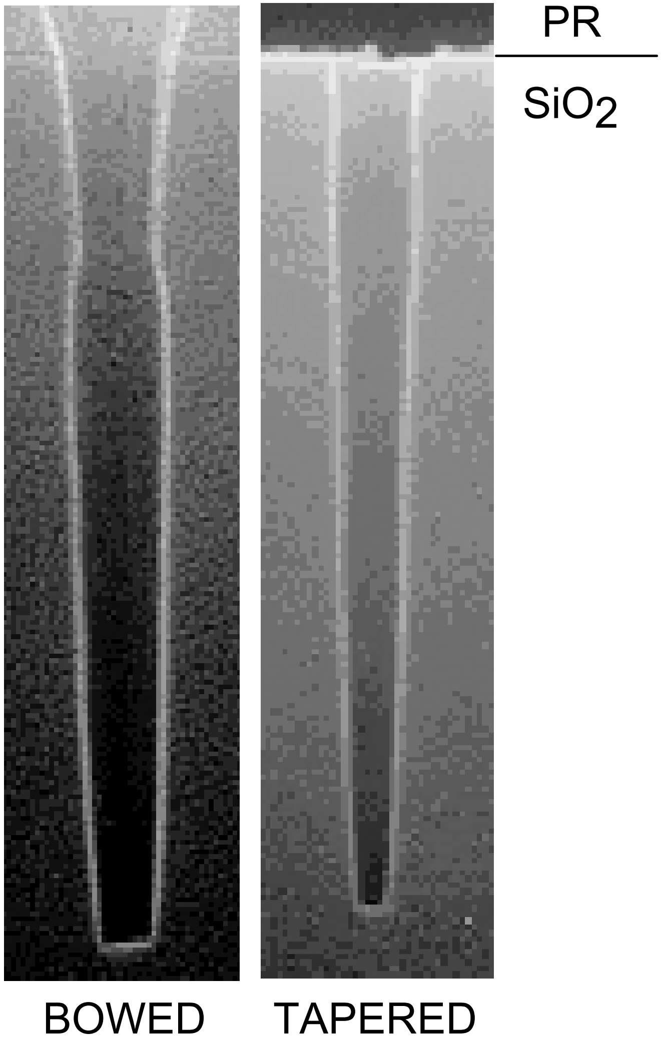

PROFILE TOPOLOGY: NEUTRAL TO ION FLUX RATIO

- **The etch profile is sensitive to the ratio of polymer forming fluxes to energy activating fluxes. Small ratios result in bowing, large ratios tapering.**

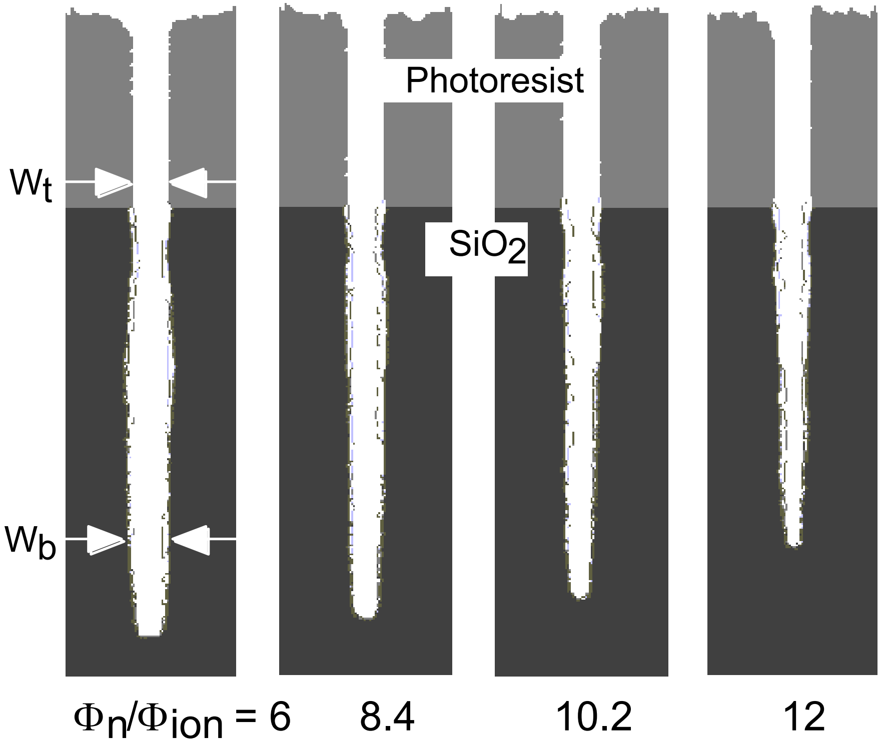

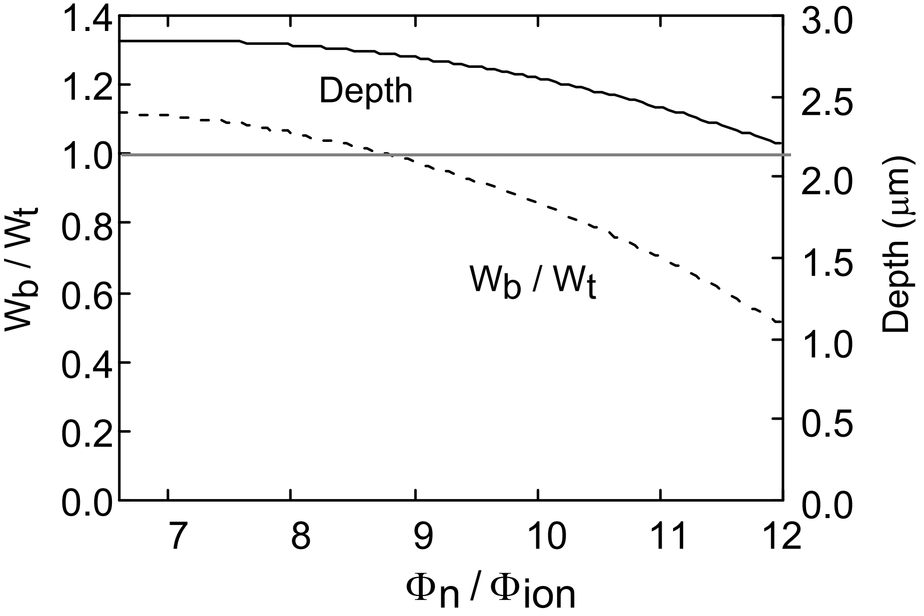

PROFILE TOPOLOGY: ENGINEERING SOLUTIONS

- Knowledge of the fundamental scaling parameter for controlling sidewall slop enables engineering solutions and real-time-control options.
- Example: Ar/C_2F_6 ratio controls polymerizing/ion flux ratio, and hence profile topology.

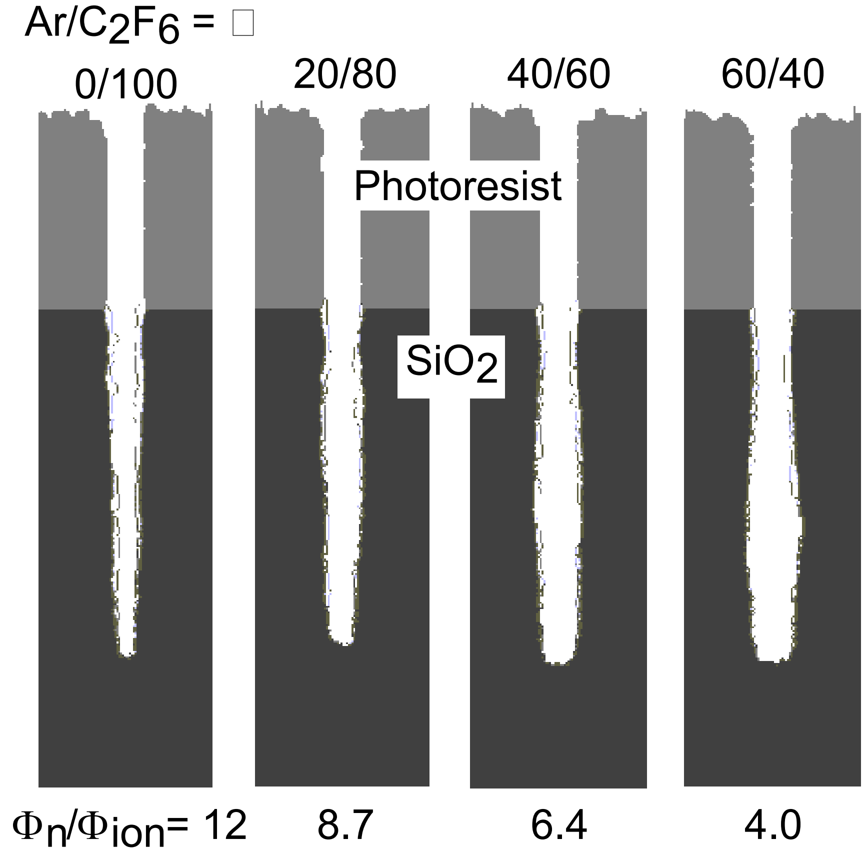

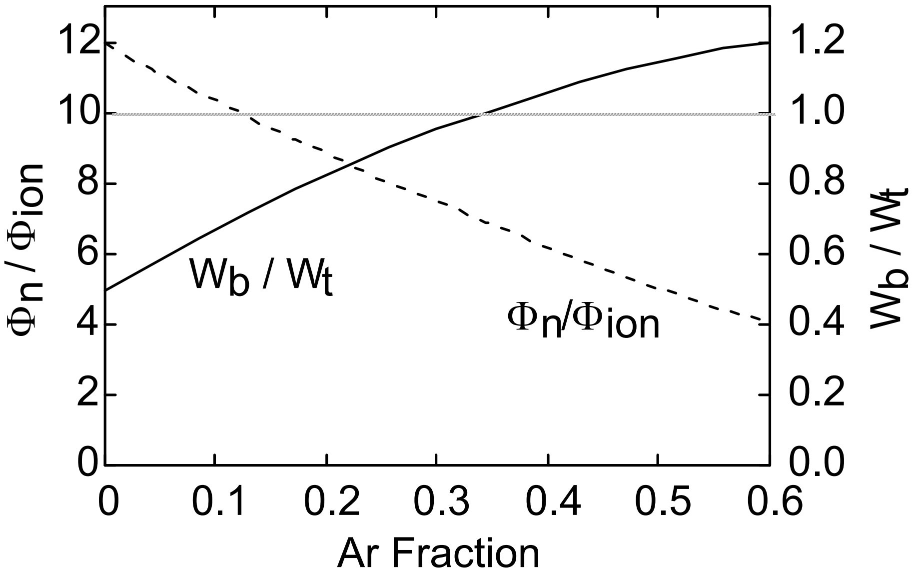

ASIDE ON REACTION MECHANISMS

- **Lack of fundamental parameters often requires calibration of models using design of experiment methodologies. In turn, the dominant, rate limiting processes are determined.**

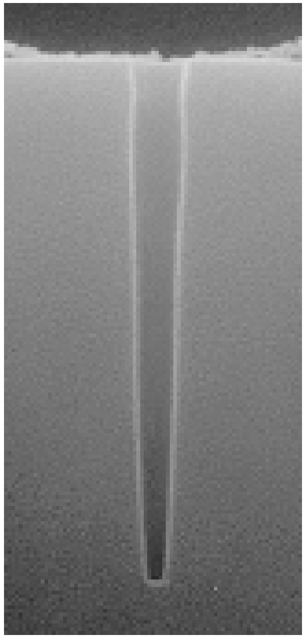

Experiment
(C. Cui, AMAT)

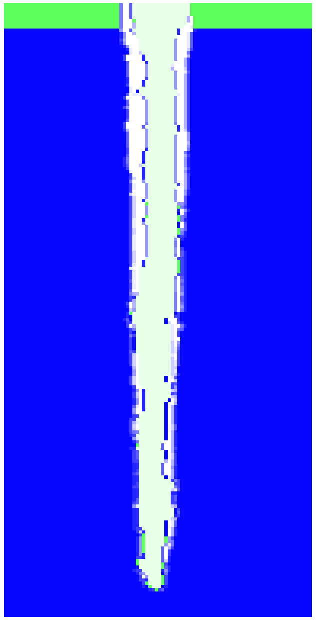

Simulation

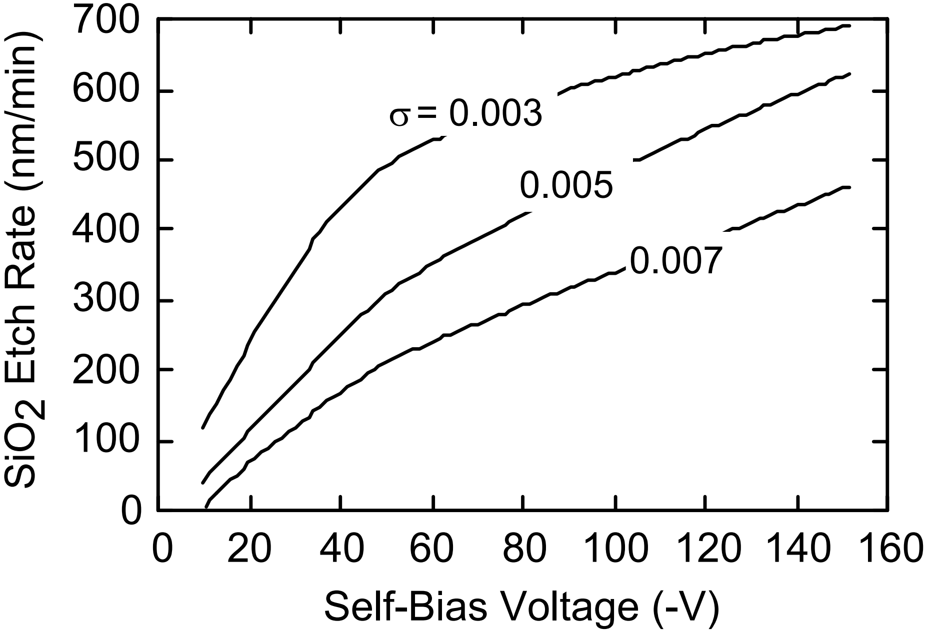

- **Parameterization of CF_2 sticking probability**

Ar/C_2F_6 = 20/80, 1000 W ICP, 150 V bias

ASIDE ON REACTION MECHANISMS

- **A *reaction mechanism* is simply a set of reactions with fundamental coefficients and probabilities which *should not depend* on the chemistry (e.g., CHF_3 vs C_2F_6 vs C_4F_8)**
- **The chemistry merely determines the magnitude of the fluxes but not the reaction pathways.**
- **An etch mechanism valid for C_2F_6 plasmas should, with no change, also be valid for C_4F_8 plasmas.**
- **Development of reaction mechanisms across different chemistries should *result in more reliable mechanisms*.**

CALIBRATION OF REACTION MECHANISM: I

- **The mechanism was validated by comparison to experiments by Oehrlein *et al* using C_2F_6 gas chemistry.[1]**

- **Threshold for SiO_2 etching was well captured at self-bias ≈ 20 V. For Si the etch rates were lower due to thicker polymer.**

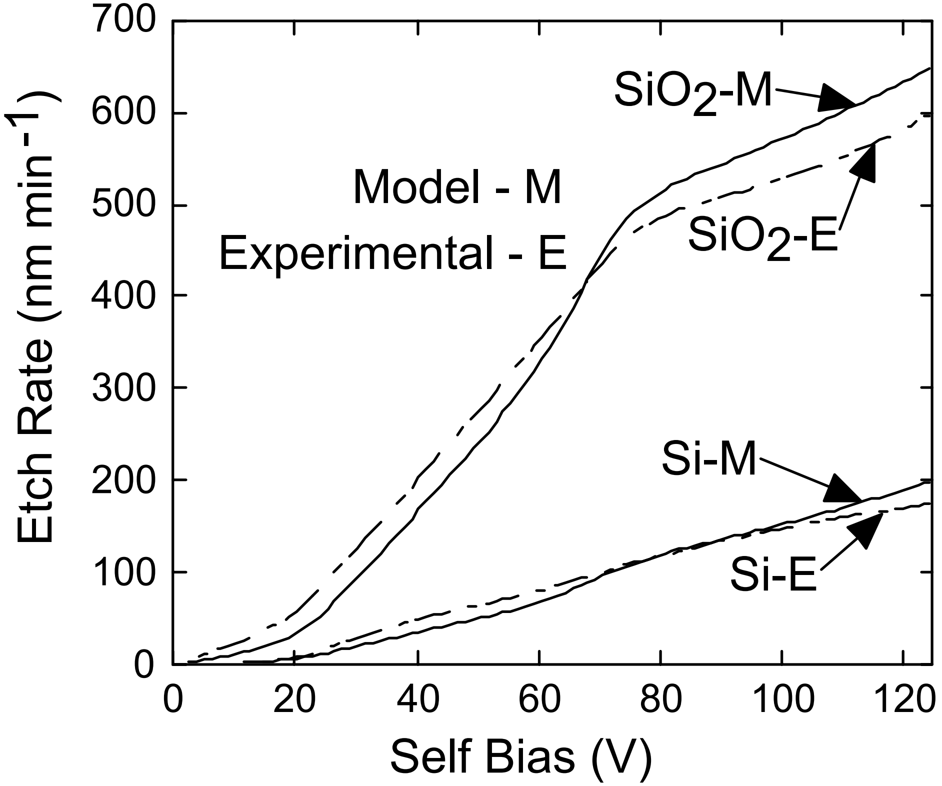

---

[1] J. Vac. Sci.Technol. A **17**, 26 (1999)

CALIBRATION OF REACTION MECHANISM: II

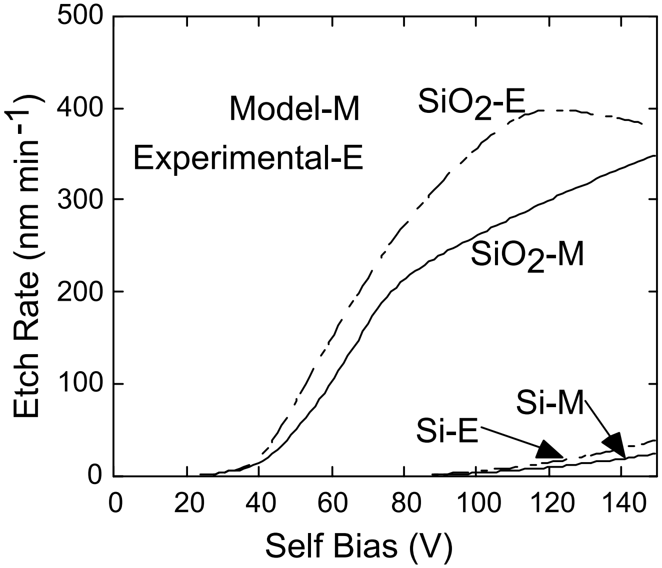

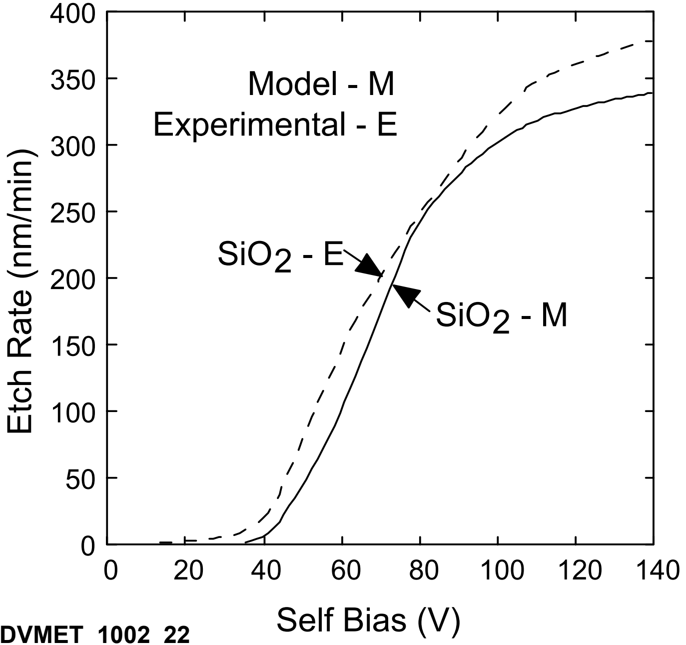

- **Threshold for SiO_2 and Si etching were well captured at for CHF_3.**
- **Differences between model and experiments for SiO_2 are attributed to H radicals forming hydrocarbon polymer chains.**
- **This is accounted for in the model by modifying sputtering rates to account for mass differences.**

WHAT CHANGES WITH POROUS SiO_2?

- **The "opening" of pores during etching of P-SiO_2 results in the filling of the voids with polymer, creating thicker layers.**
- **Ions which would have otherwise hit at grazing or normal angle now intersect with more optimum angle.**

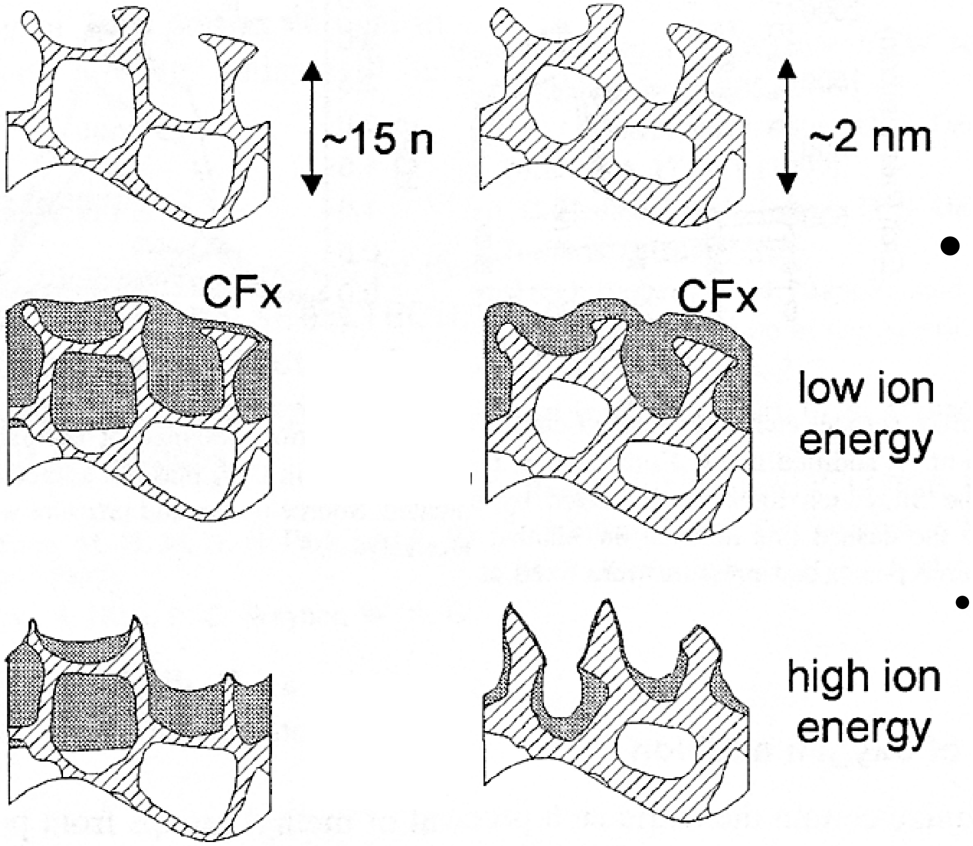

- **An important parameter is L/a (polymer thickness / pore radius).**

- **Adapted: Standaert, JVSTA 18, 2742 (2000)**

ETCH PROFILES IN SOLID AND POROUS SiO_2

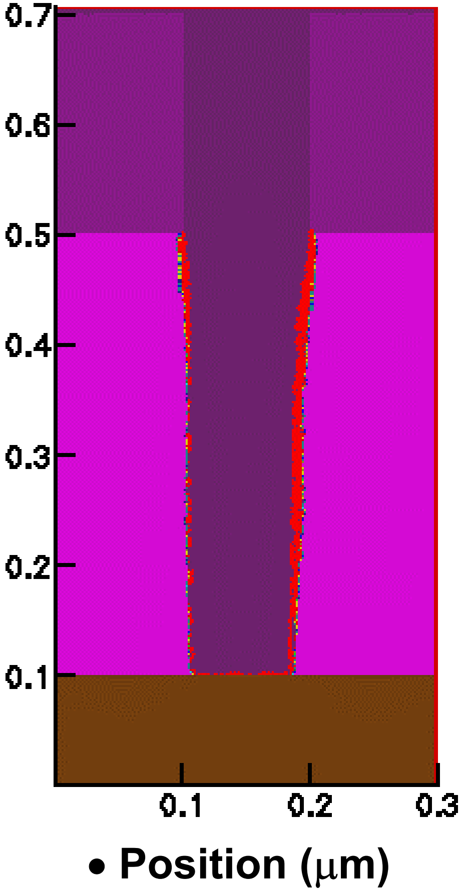

- Solid

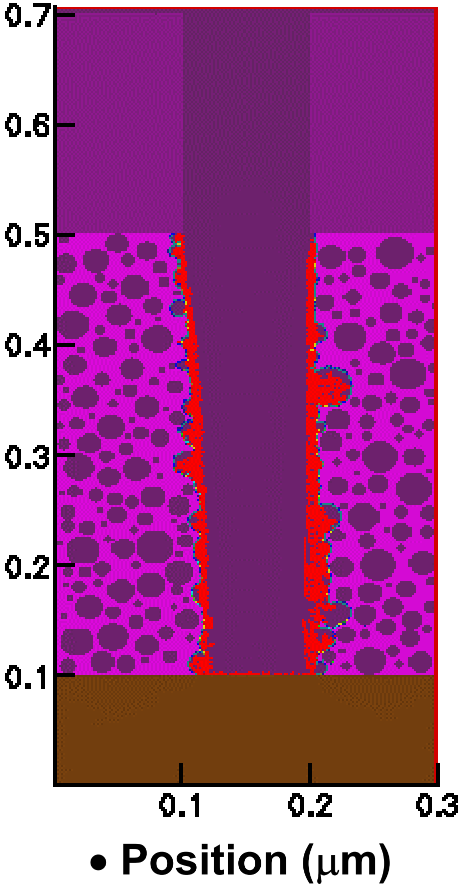

- Porosity = 45 %
  Pore radius = 10 nm

- Porous SiO_2 is being investigated for low-permittivity dielectrics for interconnect wiring.
- In polymerizing environments with heavy sidewall passivation, etch profiles differ little between solid and porous silica.
- The "open" sidewall pores quickly fill with polymer.

ETCHING OF POROUS SiO_2

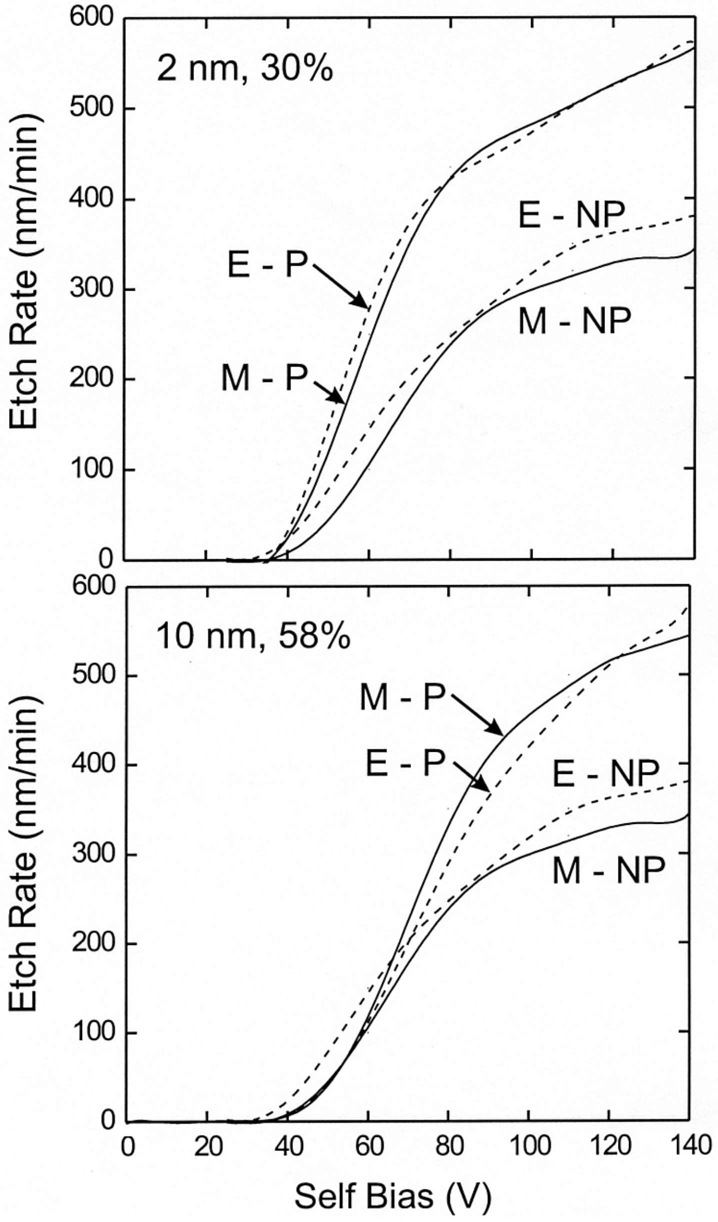

P - Porous
NP - Non porous
E - Experimental
M - Model

- **Etch rates of P-SiO_2 are generally higher than for non-porous (NP).**
- **Examples:**
  - **2 nm pore, 30% porosity**
  - **10 nm pore, 58% porosity**
- **Higher etch rates are attributed to lower mass density of P-SiO_2.**
- **CHF_3 10 mTorr, 1400 W**

Exp: Oehrlein et al. Vac. Sci.Technol. A **18**, 2742 (2000)

PORE-DEPENDENT ETCHING

- To isolate the effect of pores on etch rate, corrected etch rate is defined as

$$\text{Etch Rate (ER)}_{\text{corrected}} = \text{ER}_{\text{regular}} \times (1 - p),$$

$$p = \text{porosity}$$

- If etching depended only on mass density, corrected etch rates would equal that of NP- SiO_2.
- 2 nm pores $L/a \geq 1$: C-ER > ER(SiO_2). Favorable yields due to non-normal incidence may increase rate.
- 10 nm pores $L/a \leq 1$: C-ER < ER(SiO_2). Filling of pores with polymer decrease rates.

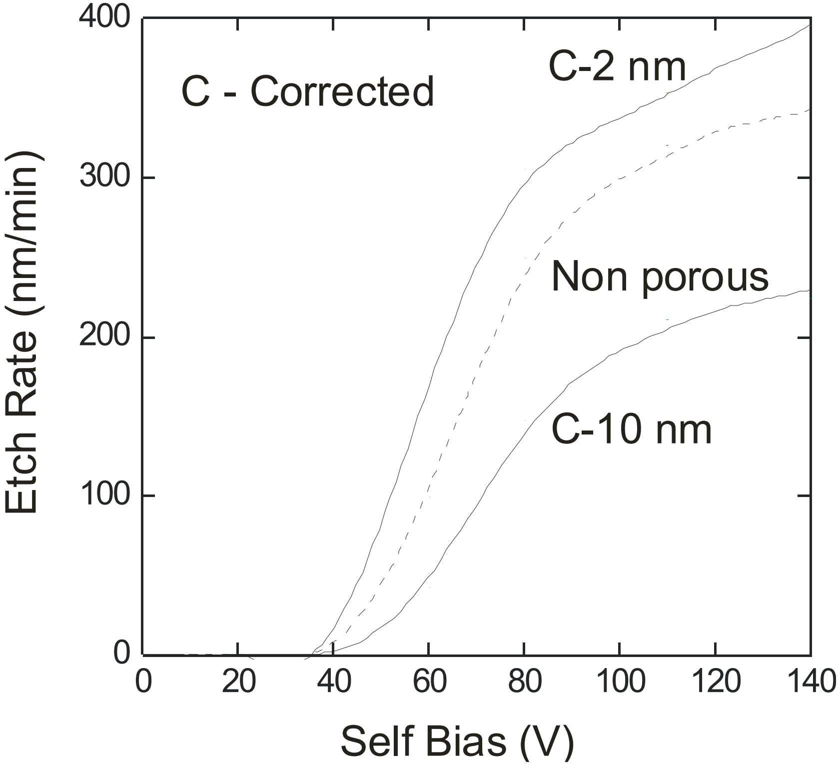

EFFECT OF POROSITY ON BLANKET ETCH RATES

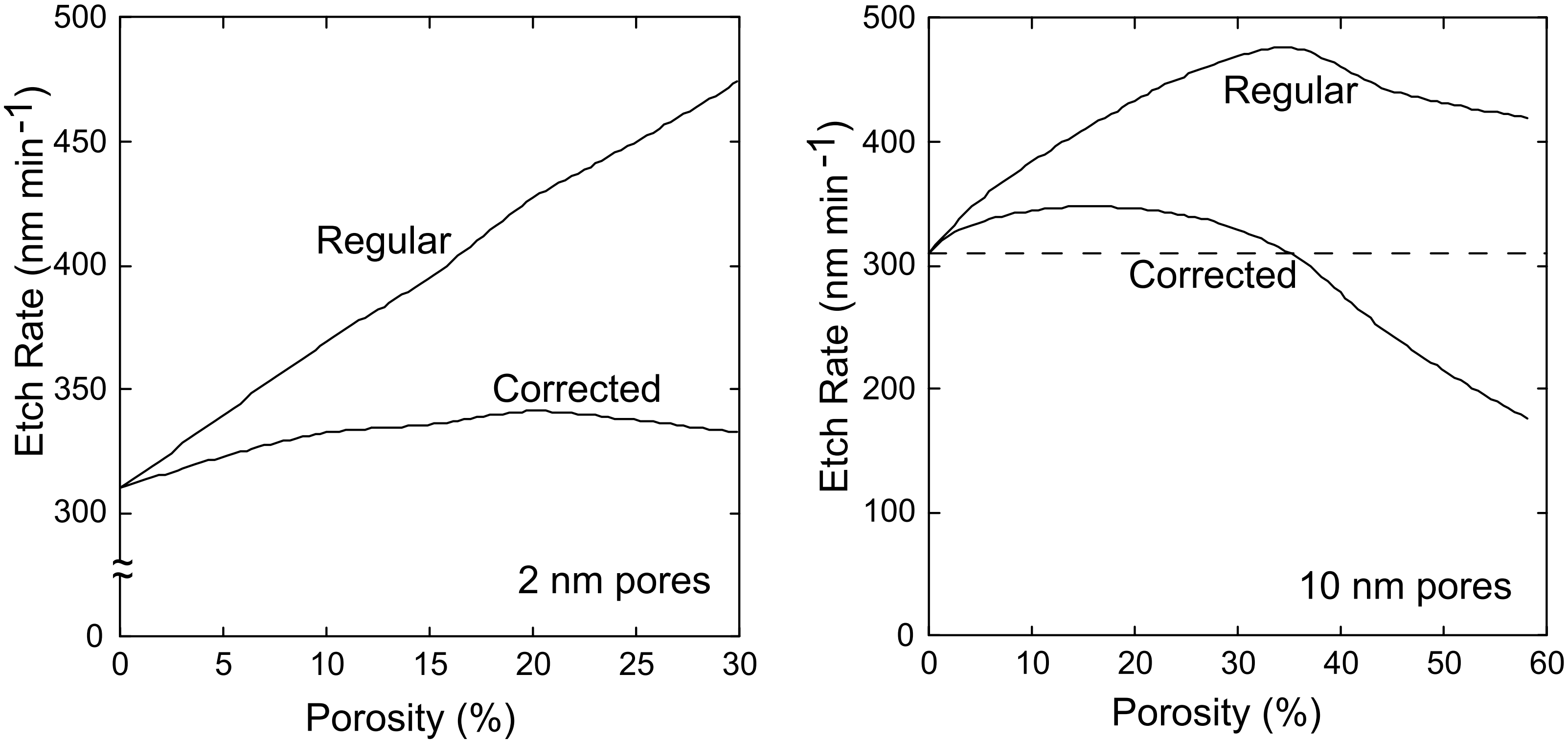

- **2 nm pores: Etch rate increases with porosity.**
- **10 nm pores: Polymer filling of pores reduces etch rate at large porosities.**

University of Illinois
Optical and Discharge Physics

EFFECT OF POROSITY ON HAR TRENCHES

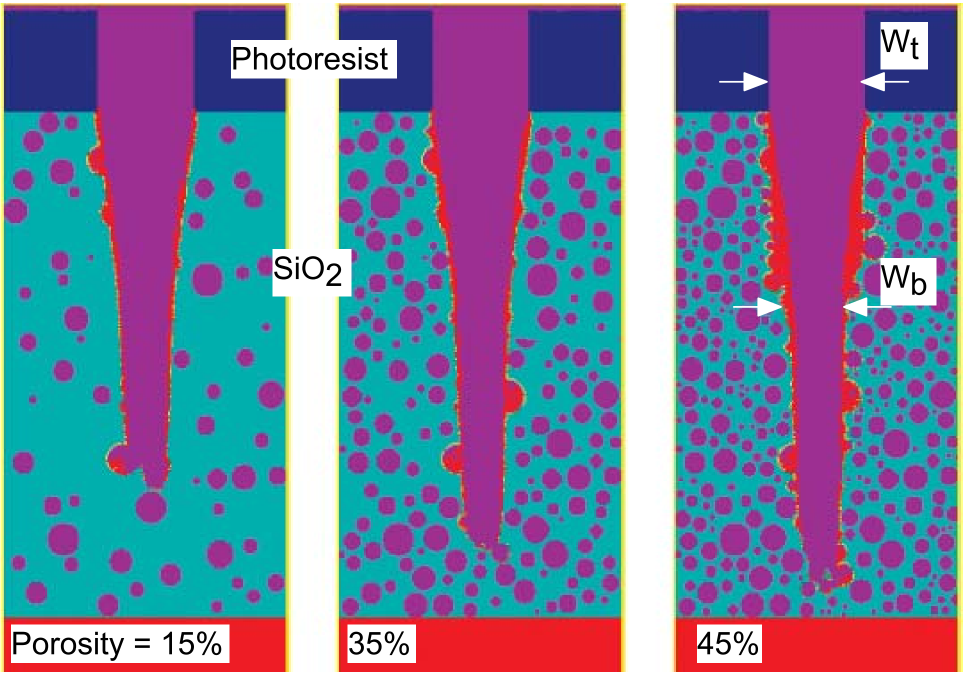

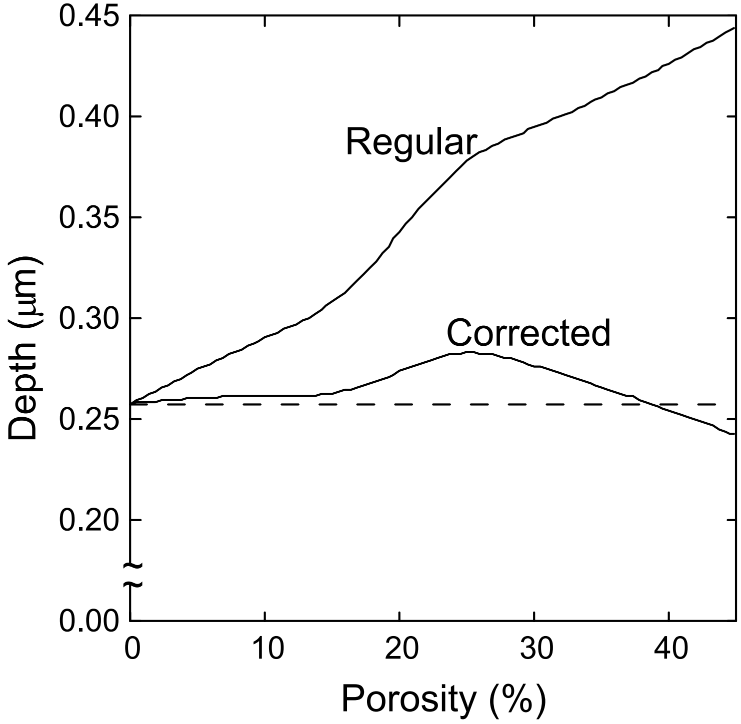

- **10 nm pores. W_t = 0.1 μm**

- **At higher porosities, more opportunity for pore filling produces thicker average polymer layers and lower etch rates.**
- **Corrected etch rates fall below SiO_2 rates when critically thick polymer layers are formed.**

EFFECT OF ϕ_n / ϕ_{ion} ON HAR TRENCHES

- **ϕ_n = total neutral flux**
- **ϕ_{ion} = total ion flux**
- **Small values of ϕ_n / ϕ_{ion} may be polymer starved, producing lower etch rates.**
- **Medium and large ϕ_n / ϕ_{ion} produces thicker polymer, lower etch rates.**
- **Increasing ϕ_n / ϕ_{ion} produces increasing taper.**

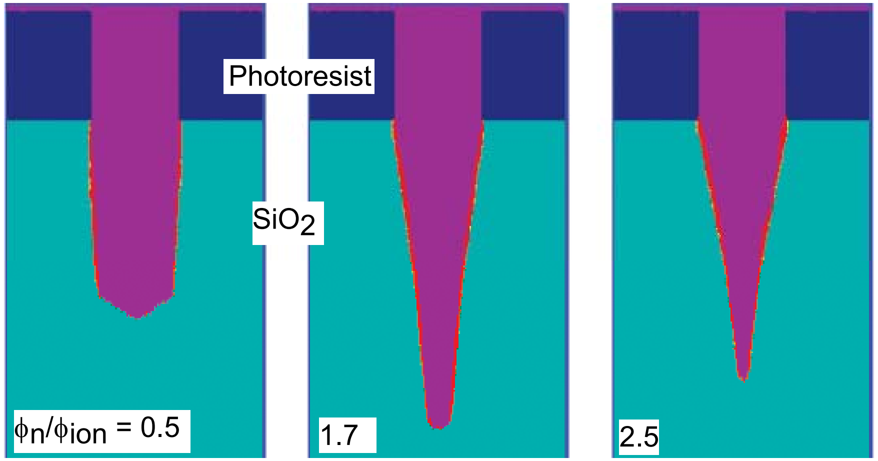

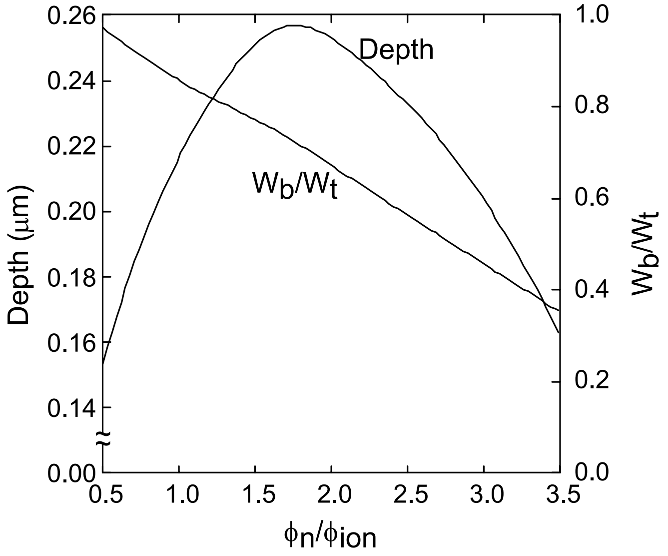

EFFECT OF ϕ_n / ϕ_{ion} ON POROUS HAR TRENCHES

- 2 nm pores.
- P- SiO_2 is more sensitive to the consequences of varying ϕ_n / ϕ_{ion} compared to NP-SiO_2.
- For large values of ϕ_n / ϕ_{ion} previously enhanced etch rates (for small pores) become depressed until etching finally stops.
- Once tapering begins the L/a increases disproportionately quickly.

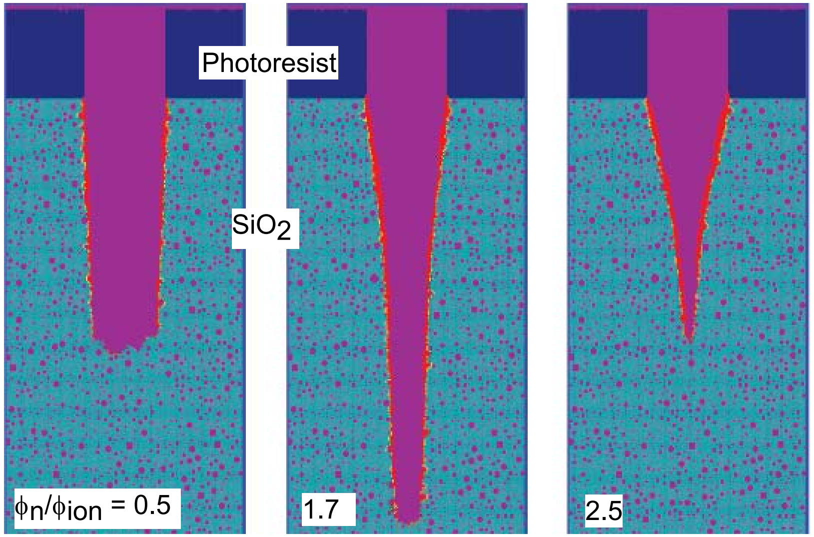

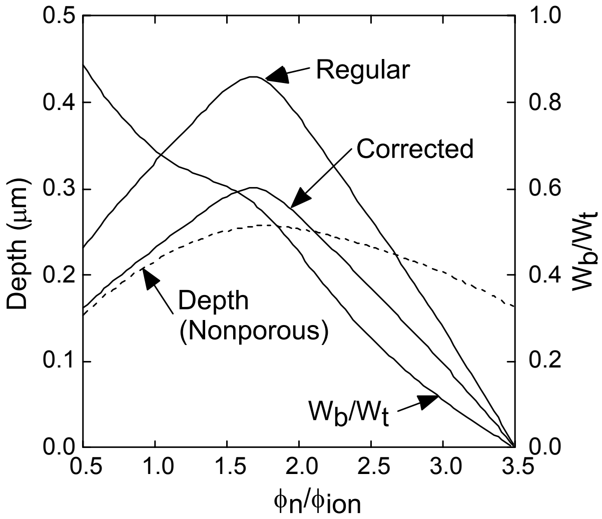

University of Illinois
Optical and Discharge Physics

EFFECT OF PORE RADIUS ON HAR TRENCHES

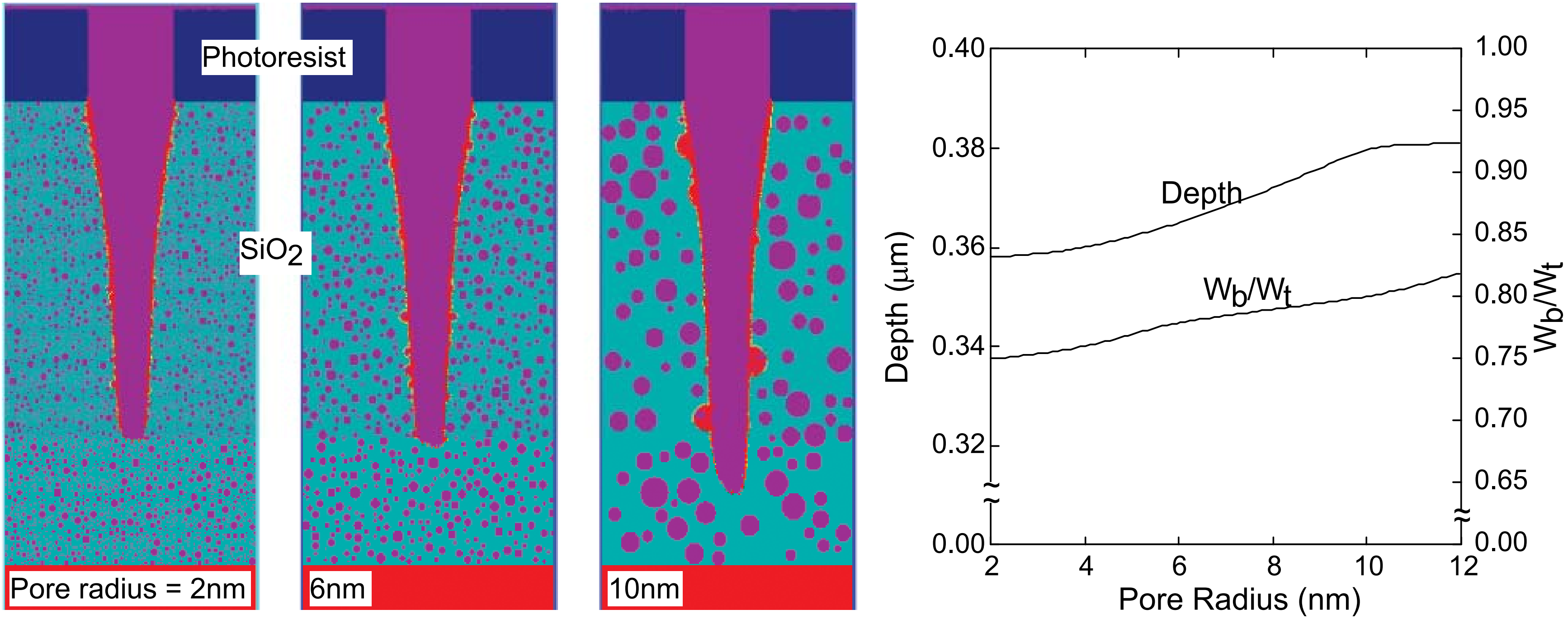

- **Porosity 25%. For sufficiently low porosity is little change in the etch rate or taper with pore radius.**

CONCLUDING REMARKS

- Etching of porous silicon-dioxide obeys many of the same scaling laws as solid materials.

- Net enhancements are seen with low porosity; net slowing of the etch rate occurs with large porosity (or pore size).

- The ratio of polymer thickness-to-pore size appears to determine much of this behavior. Thin polymer layers which fill pores appear to be thicker.

- Increased sensitivity to small changes in neutral-to-ion ratios could make maintaining CDs more problematic.